AD_____

Award Number: DAMD17-99-1-9341

TITLE: Development of KGF Antagonist as a Breast Cancer Therapeutic

PRINCIPAL INVESTIGATOR: Yasuro Sugimoto, Ph.D.

CONTRACTING ORGANIZATION: The Ohio State University Research Foundation
Columbus, Ohio 43210-1063

REPORT DATE: July 2003

TYPE OF REPORT: Final

PREPARED FOR: U.S. Army Medical Research and Materiel Command
Fort Detrick, Maryland 21702-5012

DISTRIBUTION STATEMENT: Approved for Public Release;
Distribution Unlimited

REPORT DOCUMENTATION PAGE

Form Approved
OMB No. 074-0188

1. AGENCY USE ONLY (Leave blank)	2. REPORT DATE	3. REPORT TYPE AND DATES COVERED
	July 2003	Final (1 Jul 1999 - 30 Jun 2003)

4. TITLE AND SUBTITLE
Development of KGF Antagonist as a Breast Cancer Therapeutic

5. FUNDING NUMBERS
DAMD17-99-1-9341

6. AUTHOR(S)
Yasuro Sugimoto, Ph.D.

7. PERFORMING ORGANIZATION NAME(S) AND ADDRESS(ES)
The Ohio State University Research Foundation
Columbus, Ohio 43210-1063

E-Mail: sugimoto.4@osu.edu

8. PERFORMING ORGANIZATION REPORT NUMBER

9. SPONSORING / MONITORING AGENCY NAME(S) AND ADDRESS(ES)
U.S. Army Medical Research and Materiel Command
Fort Detrick, Maryland 21702-5012

10. SPONSORING / MONITORING AGENCY REPORT NUMBER

11. SUPPLEMENTARY NOTES
Original contains color plates: All DTIC reproductions will be in black and white.

12a. DISTRIBUTION / AVAILABILITY STATEMENT
Approved for Public Release; Distribution Unlimited

12b. DISTRIBUTION CODE

13. ABSTRACT (Maximum 200 Words)
This grant proposal was to synthesize potential KGF antagonists which will then be evaluated for efficacy in in vitro assay systems. The results generated for the proposed study would be useful for designing new therapeutic agent for breast cancer.
We were able to show some potential intracellular KGFR target small molecules whereas extracellular target synthetic peptide antagonist was not able to do during this period. We also added a new dimension to an estrogen-KGF involved human breast microenvironment (i.e. KGF regulates estrogen receptor α mRNA and protein expression).

14. SUBJECT TERMS
No Subject Terms Provided.

15. NUMBER OF PAGES
34

16. PRICE CODE

17. SECURITY CLASSIFICATION OF REPORT	18. SECURITY CLASSIFICATION OF THIS PAGE	19. SECURITY CLASSIFICATION OF ABSTRACT	20. LIMITATION OF ABSTRACT
Unclassified	Unclassified	Unclassified	Unlimited

Table of Contents

Introduction:

This grant proposal is to synthesize potential KGF antagonists which will then be evaluated for efficacy in *in vitro* assay systems. The results generated for the proposed study will be useful for designing new therapeutic agent for breast cancer.

Body:

Development of KGF antagonist as a breast cancer therapeutic agent

Task 1: Synthesis of nine hexacosapeptides as KGF antagonists

As reported in previous progress report, KGF antagonist candidate peptides have been synthesized (Table 1). Stably-transfected MCF-7 and MDA-MB-231 cells with KGF were also established. The stably transfected MCF-7 cells with KGF (MCF-7-KGF) were used for a ^{3}H-thymidine incorporation assay and aromatase activity assay. However, significant inductions of ether DNA-synthesis or aromatase activity were not observed by KGF treatment. The stably transfected MDA-MB-231 cells with KGF (MDA-MB-231-KGF) were also examined, however, significant positive induction of either DNA-synthesis or aromatase activity were not observed by KGF treatment. A receptor-binding assay was also performed using MCF-7-KGF, however, neither a competitive binding assay nor cross-linking assay drowned a reportable positive result. The P.I., then thought that a reason of these series of failures might be a lack of sensitivity, in other word, low KGF-receptor (KGFR) expression in those cells. Therefore, we decided to establish a KGFR overexpressed breast cancer cell line. A mouse KGFR cDNA cloned in a mammalian expression vector was obtained from Dr. Pui-Kai Li, The Ohio State University, and the plasmid was transfected into the NIH-3T3 mouse fibroblast cells, MCF-7, MDA-MB-231 and T47D breast cancer cells.

A. Effect of KGF on cell proliferation in MCF-7 cells transfected with KGFR

The MCF-7 cells transfected with KGFR plasmid (MCF-7-KGFR) was G-418 antibiotics-selected, and elevated KGFR mRNA and its protein levels were verified. Cells were plated at a density of 0.5×10^4 in 24-well plates in a volume of 1 ml/well. After the cells were attached to the wells, the medium was replaced with 1 ml of fresh DMEM/F12 with 0.02% BSA (basal medium). In 24-hours, medium was replaced with the basal medium containing increasing amount of KGF. At the end of 24-hour KGF treatment, cells were pulsed with 1mCi/ml [^{3}H] methyl thymidine for 3 hours. Cells were washed, fixed and rinsed prior to lysing in the NaOH solution. Cell lysate was neutralized and submitted for a radioactivity measurement in a Scintillation counter. As shown in Figure 1, KGF significantly stimulates DNA synthesis in MCF-7KGFR at 1ng/ml.

Figure 1. Effect of KGF on DNA synthesis in KGFR-overexpressed MCF-7 cells

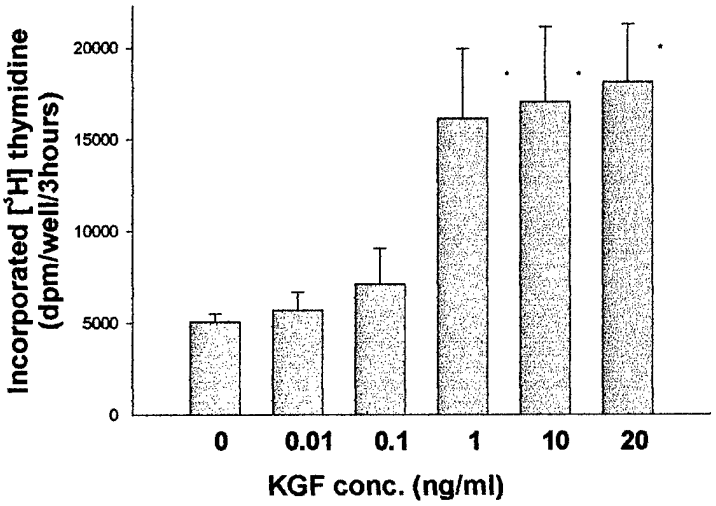

Results: Although as high as 100μM of each peptide was used to inhibit the stimulation of DNA synthesis by 5ng/ml KGF treatment in MCF-7-KGFR cells cultured in DMEM/F12 with 0.02% BSA (basal medium), only *pep*KGF4, *pep*KGF 5 and

*pep*KGF 9 showed less than 10% inhibition. None of them were significant. To date, we have not been able to figure out the reason of its disability of blocking the KGF-KGFR interaction. We speculate that involvement of heparin in KGF-KGFR complex makes a difference. There are numbers of reports that describe an involvement of heparin in this complex. However, at least in our culture system addition of various concentration of heparin did not alter the outcome results on inhibition assay. The study in this issue is in progress.

Table 1. Peptide Amino Acid Sequence

pepKGF1	KGF_{31-56}	ACNDMTPEQMATNVNCSSPERHTRSY
pepKGF2	KGF_{48-73}	SPERHTRSYDYMEGGDIRVRRLFCRT
pepKGF3	KGF_{65-90}	RVRRLFCRTQWYLRIDKRGKVKGTQE
pepKGF4	KGF_{82-107}	RGKVKGTQEMKNNYNIMEIRTVAVGI
pepKGF5	KGF_{99-124}	EIRTVAVGIVAIKGVESEFYLAMNKE
pepKGF6	$KGF_{116-141}$	EFYLAMNKEGKLYAKKECNEDCNFKE
pepKGF7	$KGF_{133-158}$	CNEDCNFKELILENHYNTYASAKWTH
pepKGF8	$KGF_{150-175}$	TYASAKWTHNGGEMFVALNQKGIPVR
pepKGF9	$KGF_{168-194}$	NQKGIPVRGKKTKKEQKTAHFLPMAIT

B. KGFR specific antibody: To date, only few KGFR-related antibodies are available commercially (*e.g.* SC-6930 and SC-122, Santa Cruz, SD). Since these receptor antibodies are raised against a peptide mapping at the carboxy terminus of Bek receptor (also designated KGFR or FGFR-2), these antibodies can recognize not only KGFR but also other FGFR-2 isoformes (to date, at least 13 isomers are known). As it is reported KGF has high affinity to KGFR and very low affinity to other FGFR family if it is not no-affinity. In order to eliminate the cross-reactivity of the antibody with other FGFR-2 isoforms and other FGFR family, we have designed and generated KGFR specific antibody and its specificity was examined thoroughly. KGFR extra cellular domain specific rabbit polyclonal antibody - it was raised against a peptide mapping at thethird Ig-like domain of KGFR of human origin (identical to corresponding mouse sequence). The KGFR specific peptide used for this purpose was as follows: HisSerGlyIleAsnSerSerAsnAlaGlu. This amino acid sequence is a part of the KGFR specific region, 38 amino acids as follows: (HSGINSSNAEVLALFNVTEADAGEYICKVSNYIGQANQ). This sequence was analyzed by computer software with the following factor as parameters and narrowed to a suitable 10 amino acid for the antisera production: Hydrophilicity: Kyte-Doolittle, Antigenic index: Jameson-Wolf, Surface probability: Emini, Flexible regions: Karplus-Schulz, Alpha-Amphyipathic region: Eisenberg, Beta-Amphyipathic region: Eisenberg. Alpha, beta, turn, or coil resions: Garnier-Robson, and Chou-Fasman. The antibody produced were used not only for development of a cellular kinase assay method, describe below, but also for immunohistochemistry analysis of KGFR expression in breast cancer tissue specimen obtained through the tissue procurement service at the OSU comprehensive cancer center. We are on a process of obtaining the data to explain the correlation of KGFR protein expression and breast cancer grade, age, and/or other parameters by using this KGFR specific antibody.

Immunohistochemistry was performed on paraffinsections (5 μm) dewaxed in xylene and rehydrated indecreasing concentrations of ethanol. Endogenous peroxidase was inactivated with 3% hydrogen peroxidefor 5 min, and nonspecific binding was blocked by incubation in 5% normal goat serum for 20 min. The sections were stained for KGFR by using VECTASTAIN® Universal Quick Kit and DAB Substrate Kit, according to the manufacturer's instructions. The primary KGFR antibody was an affinity-purified rabbit polyclonal antibody produced as mentioned above. An optimal primary antibody dilution of 1:1000 was determined by titration in this system, and omission of primary antibody served as a negative control.

Figure 2. Immunohistochemical staining analysis of a breast cancer patient

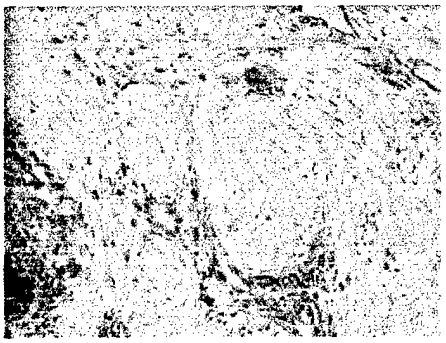

KGFR

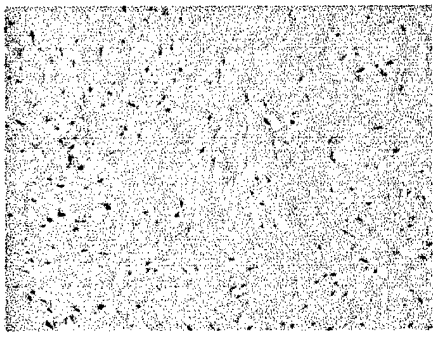

Control

As shown in the Figure 2, Immunohistochemical staining revealed that human breast cancer tissue has high intensity staining of KGFR in the epithelial compartment. This result supports our previously reported results that KGFR mRNA exclusively expressed in epithelial cells.

We have also generated a KGFR specific polyclonal antibody. *KGFR intracellular tyrosine kinase (TK) domain specific polyclonal antibody* - was raised against a peptide mapping at the second TK domain of KGFR of human origin (identical to corresponding mouse sequence). The KGFR specific peptide used for this purpose was as follows: AspIleAsnArgTyrProGluGluGlnMetThrPhe. Same procedure with previously described KGFR specific sequence analysis method was used to specify the antigenic peptide. The antibodies were generated by contracted third party under our supervision and the titration has been determined (1 to 80,000). The specificity of this KGFR antibody was analyzed as follows: The whole cell protein extracted from the stably transfected NIH-3T3 cells with KGFR was used for Western blotting analysis. We observed that the antibodies recognized the 115kD KGFR protein. However, extra nonspecific bands were also recognized. Therefore we did not utilize this *KGFR intracellular TK domain specific polyconal* antibody for further studies.

C. Solid phase receptor binding assay: Assaying the binding characteristics of KGF antagonists to the KGFR would permit the selection of the synthetic KGF antagonist with both high affinity for KGFR and the ability to suppress KGF activity.

KGFR over expressed protein: The extra cellular domain of KGFR cDNA was RT-PCR-cloned by using the following pair of primers: 5'-ACCATGGTCAGCTGGGGTCGTTTCATCTGCCT-3' and 5'-

CTCCAGGTAGTCTGGGGAAGCTGTAATCTCC-3'. The amplicons of KGFR extra cellular domain cDNA was cloned into a mammalian gene express vector pEF6/V5-His-TOPO. A clone was DNA sequenced and verified the orientation. This clone, pEF6/V5-His-KGFR, was used for the establishment of stably transfected cells with KGFR-overexpression plasmid (pEF6/V5-His-KGFR). A human breast cancer cell line T47D was transfected with the pEF6/V5-His-KGFR plasmid and then the stably transfected cells were selected by using the Blasticidin antibiotics serection. The overexpressed cells were cultured and the condition medium was collected twice a week to pool. The pooled medium was used for the overexpressed KGFR-extracellular membrane portion purification. Since the overexpressed protein has a stretched His (6xHis) in the –COOH terminal of its protein, it was purified by using a Nickel-Chelationg resin.

After the extracellular portion of V5 tagged-KGFR protein was collected and purified, the well surface was coated with anti-V5 polyclonal antibody (Invitrogen) overnight. After washing and blocking the well, the purified V5 tagged-KGFR fragment protein (100ng) was applied to the wells. A 0.4ng of ^{125}I-KGF was applied along with an increasing amount of KGF antagonist described above. After 2-hour incubation, the wells were washed thoroughly; minimum amount of 0.2M NaOH was applied to dissolve all remaining molecules. The radioactivity was measured by using a gamma counter. The receptor binding inhibition efficacy was expressed as followed: The specific binding of KGF to KGFR was obtained in the absence of peptide antagonists were taken as 0% inhibition. A 100 ng of KGFR extracellular fragment protein was incubated with various concentrations of a synthetic peptide with ^{125}I-rKGF, and its IC50 was calculated.

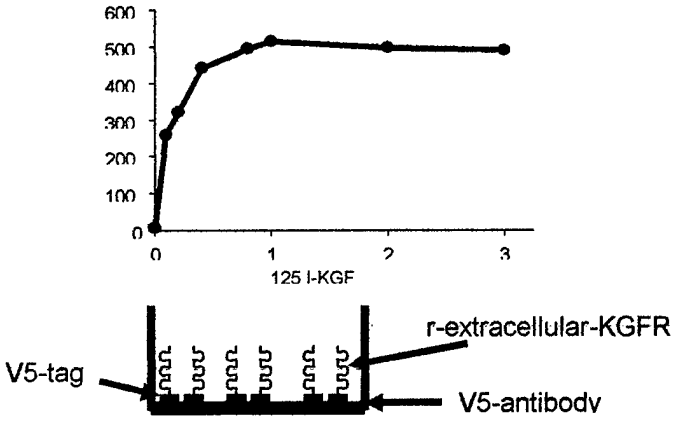

Figure 3 and 4. Solid phase binding assay

A datum obtained from this assay (Figure 3, above) and the simplified assaying system (Figure 4, below)

Similar to the results described in the section A, no significant competitive binding of any peptides with [^{125}I]-rKGFR were observed. In this study we tested the ability of peptides listed in the Table 1 to displace [^{125}I] KGF from the recombinant extracellular KGFR coated on V5-antibody to localize the KGFR binding site on KGF. Displacement by unlabeled KGF was 50% at about 2 ng/mL. Only *pep*KGF4, *pep*KGF 5 and *pep*KGF 9 weakly displaced [^{125}I]-rKGF in a dose-dependent manner but only at the higher concentration tested (< 50nM). These data suggest, however, far higher peptide concentrations (10^3-10^4-fold) were required relative to full-length KGF, the fact that other peptides had no effect on KGF binding even at the highest concentrations tested. However it is also true that the data obtained from *pep*KGF4, *pep*KGF 5 and *pep*KGF 9 were specific.

Taken together with the data shown in section A, only the *pep*KGF4, *pep*KGF 5 and *pep*KGF 9 have weak binging ability to KGFR and have ability to compete with the KGF for binding to KGFR.

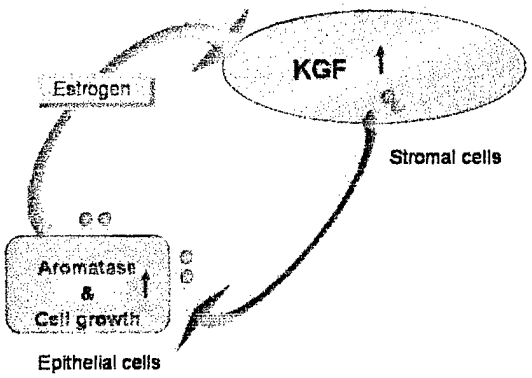

Figure 5. A positive feedback loop in breast microenvironment

Since we were unable to establish a reliable assaying system to test the synthetic peptide antagonists, we tried to find other system to evaluate an ability to test them. As we have shown that there is a positive feed back system between KGF and estrogen (Figure 5).
We thought that estrogen receptor might be actively involved in this positive feedback system. Therefore we decided to test this hypothesis.

D. Effect of KGF on ERα expression regulation in human breast cells:

There are increasing amount of evidences that the ability of estrogens to induce the formation and secretion of various growth factors in established human breast cancer cell lines. We have demonstrated that keratinocyte growth factor (KGF), which is produced in stromal cells and is mitogenic for normal mammary epithelium *in vitro*, can stimulate aromatase activity and cell growth in breast primary culture cells independently with estrogens. However, the interaction among growth factors and hormone regulation within is still not well defined yet in breast cancer progression. Described here was to use MCF-7 cells as a model to explore the role of KGF in regulation of estrogen receptor-α (ER-α).

Figure 6. KGF suppresses ERα mRNA in MCF-7 cells

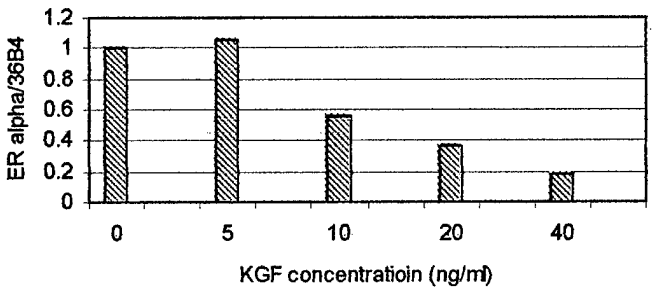

The MCF-7 cells were cultured in phenol red-free DMEM/F12 supplemented with 0.02% bovine serum albumin for 24 hours before treatment. MCF-7 cells were treated with 10 ng/ml KGF in phenol red-free DMEM/F12 supplemented with 5% dextran-coated charcoal treated fetal bovine serum for 24 hours. Controls were treated with vehicle in the same medium. The mRNA expression level of ER-α in MCF-7 cells was evaluated by Real-time quantitative PCR.

The nucleotide sequences of the hybridization probe and primers for the ER-α and 36B4 genes are as follows: ER-α: 5'-AGCTCCTCCTCATCCTCTCC-3', 5'-TCTCCAGCAGCAGGTCATAG-3' and FAM-TCAGGCACATGAGTAACAAAGGCA-TAMRA, and 36B4: 5'-CTGGAGACAAAGTGGGAGCC-3', 5'-

TCGAACACCTGCTGGATGAC-3' and FAM-ACGCTGCTGAACATGCTCAACATCTCC -TAMRA

Relative quantitation of ER-α expression and Real-time PCR:

The comparative CT method was used for the relative quantitation of ER-α. The parameter CT (threshold cycle) is defined as the fractional cycle number at which the fluorescence generated by cleavage of the TaqMan® probe-amplicon complex formation passes a fixed threshold above baseline. The relative ER-α mRNA expression level was expressed as $2^{-(\Delta CT \text{ sample} - \Delta CT \text{ control})} = 2^{-(\Delta \Delta CT)}$. The ΔCT was a normalized value of ER-α CT value to the endogenous control of 36B4 CT value. All PCR reactions were performed using an ABI Prism 7000 Sequence Detection System (Perkin-Elmer Applied Biosystems).

Western Blot Analyses:

Total proteins were extracted from MCF-7 cells. Protein samples were separated on 4 -15% Tris-HCl Ready Gel (BIO-RAD laboratories, Hercules, CA) and transferred onto polyvinylidene fluoride (PVDF) membranes (Millipore, Bedford USA) and was visualized with a chemiluminescent detection system (ECL; Amersham Pharmacia Biotech, Piscataway, NJ) and exposed on Hyperfilm™ ECL™ (Amersham Pharmacia Biotech, Piscataway, NJ)

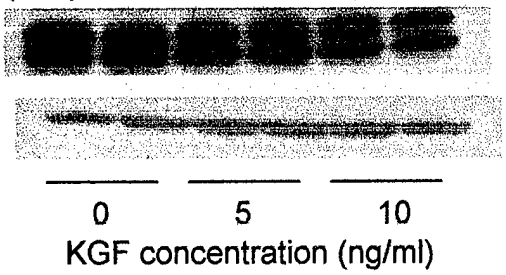

Figure 7. KGF suppresses ERα protein in MCF-7 cells

KGF treatment of MCF-7 cells suppressed ER-α mRNA expression in a dose dependent manner. KGF supressed ER-α mRNA expression levels by 35- 50%. Our results indicated that KGF down-regulates ER-α mRNA expression in MCF-7 cells. The protein level also suppressed by KGF treatment. Examination of growth factor regulation of the ER-α in the MCF-7 cells suggests that altered hormonal responses could be due to down-regulation of ER-α. These data have implication for the role of exposure to KGF in the control of hormone independent tumor progression.

E. Measurement of KGFR mRNA expression in human breast cells

As mentioned in section B, we are evaluating the KGFR expression level of protein in the human breast tissue specimen. We have also developed an evaluation method for KGFR mRNA expression levels in primary cultured breast cells.

Human breast tissues

Normal human breast tissues and breast cancer tissues were obtained through the Tissue Procurement Program of The Ohio State University Hospital. At the time of procurement, the tissue samples were placed in a mixture of Dulbecco's Modified Eagle's Medium and Ham's F12 Medium (1 : 1) (DMEM/F12) without phenol red and stored at 4◦C before transfer to the laboratory.

Tissue dissociation Tissues were sterilized in 70% ethanol for 30s, and then washed three times with fresh DMEM/F12. Tissue samples were minced, and then dissociated overnight at 37◦C with 0.1% collagenase in phenol red-free DMEM/F12 medium(1 g tissue/ml) supplemented with 5% fetal bovine serum (FBS) and antibiotic-antimycotic (100 unit/ml penicillin G sodium, 100µg/ml streptomycin sulfate and 0.25µg/ml amphotericin B).

Cell culture The digested mixture was centrifuged at 200×g for5min at 25◦C. The cell pellet was re-suspended and allowed to settle by gravity. The supernatant (containing mostly stromal cells) was then centrifuged at 200×*g* for 5 min at 25◦C and the pelleted stromal cells were re-suspended in phenol red-free high-calcium DMEM/F12 (1.05mM $CaCl_2$) supplemented with 5% FBS. The initial sedimented cells (containing mostly epithelial cells) were washed three times with phenol red-free DMEM/F12 medium and allowed again to settle by gravity. Then, the sedimented epithelial cells were re-suspended in phenol red-free low calcium DMEM/F12 (0.04mM $CaCl_2$) supplemented with Chelex-100 (Bio-Rad Laboratories, CA) – treated FBS (10%). Adipose stromal cells were also isolated from normal human breast tissues. After initial centrifugation of the digested tissue, yellow adipose fraction was collected and suspended in phenol red-free high-calciumDMEM/F12 (1.05mM $CaCl_2$) supplemented with 5% FBS. All three isolated specific cell types were plated separately in 75-cm^2 culture flasks in a humidified incubator (5% CO_2:95% air, 37◦C). The media of all primary cultured human breast cells and human breast cancer cells were changed every 2 days. When the cells grew to confluence, cells were washed twice with calcium- and magnesium-free Phosphate Buffered Saline (PBS, pH7.3), and then trypsinized with0.5% trypsin – 5.3mM EDTA (GibcoBRL) in PBS for 10min at 37◦C. The trypsinization was stopped by addition of culture medium with 5% FBS. After centrifugation, the dissociated cells were resuspended in the same medium and subcultured into 75-cm^2 culture flasks at a ratio of 1 flask to 5 flasks. After first subculture of the cells, a part of cells were subjected for total RNA extraction.

After reverse transcription reaction was made, a cDNA equivalent to 100ng RNA was used for real-time quantitative PCR as described in the section D. Following primers and probe was used for this assay: KGFR: 5'-GGATAAATAGTTCCAATGCAGAAGTG-3', 5'-CTGCCCTATATAATTGGAGACCTTAC-3' and FAM-CCCAGCATCCGCCTCGGTCACAT-

Figure 8 and 9. Expression of KGFR mRNA in Breast

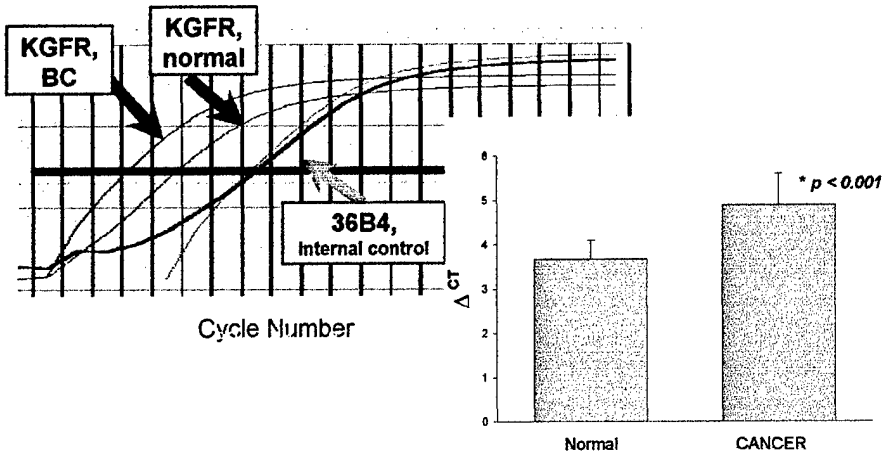

TAMRA, and 36B4: 5'-CTGGAGACAAAGTGGGAGCC-3', 5'-TCGAACACCTGCTGGATGAC-3' and FAM-ACGCTGCTGAACATGCTCAACATCTCC –TAMRA. Same analysis method was used as describe above.

Figure 8 shows an example of outcome data of this part of study. Figure 9 shows that significant mRNA expression level difference between the primary cultured epithelial cells from no-cancerous and cancerous tissue. Although the graph was drown from the data obtained from 5 patients each from each groups, the mRNA expression levels are significantly different. We are collecting the data to explain the correlation of KGFR protein expression and breast cancer grade, age, and/or other parameters by using this technique.

F. Involvement of PTPγ in the KGF-estrogen positive feedback loop in breast cancer environment

Protein tyrosine phosphatases (PTPs) play an essential role in the regulation of cell activation, proliferation and differentiation, since they counterbalance the growth-promoting effects of protein tyrosine kinases (PTKs). Therefore, alterations in PTPs activity might affect cell growth, neoplastic processes and transformation. Previous work suggests that PTPs may also be important in the growth of breast cancer and may be affected by estrogenic agonists and antagonists. Human breast tumors exhibit enhanced tyrosine kinase activity relative to benign breast disease or normal breast tissue. The growth rate of a large proportion of breast cancers is influenced by sex steroid hormones, and both steroid hormone and protein tyrosine phosphorylation is demonstrated to play important roles in cell proliferation. PTPγ is a member of the receptor-like family of tyrosine-specific phosphatases, and the structure of the receptor-like PTPs include an extracellular, a transmembrane, and one or two tandemly repeated catalytic domains. This structure implies ligand-binding capability which may modulate enzymatic activity. The putative ligands for most of the PTPs with receptor-like structures are yet to be identified. According to mRNA analysis, PTPγ is a broadly expressed enzyme that exists in many tissues, including human lung, stomach, esophagus, colon, liver, spleen, and kidney. Based on the chromosomal location of the PTPγ gene (3p14.2) and studies

Figure 10.

KGF suppresses a tumor supressor gene PTP-γ in human breast cancer cell line MCF-7

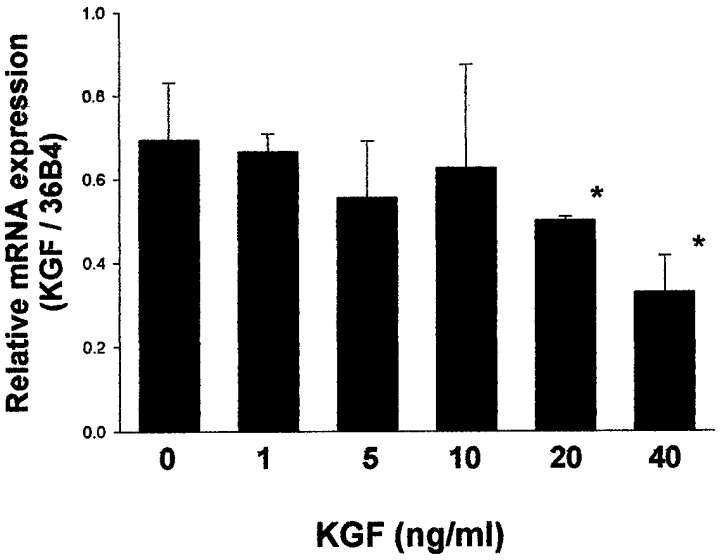

showing loss of heterozygosity of the gene in kidney tumors, PTPγ has been implicated as a candidate tumor suppressor gene. More recently, PTPγ expression levels were shown to be reduced in ovarian and lung tumors.

We have reported that the PTPγ mRNA expression was lower in cancerous than in normal breast tissues. Both E2 and Zeranol (Z) suppressed PTPγ mRNA levels in cultured normal breast tissues by 80%, but had a lesser effect in cultured epithelial cells isolated from normal breast tissues. In the co-culture system, both E2 and Z suppressed PTPγ mRNA to a greater degree in epithelial cells than in stromal cells. In whole breast tissues, PTPγ was immunolocalized to the epithelium. Treatment with E2 or Z diminished PTPγ staining indicating reductions in PTPγ at the protein level. The results indicate that both E2 and Z regulate PTPγ expression in human breast and that epithelial–stromal cells interaction is important in the regulation of PTPγ expression by estrogenically active agents.
In order to extend our understanding of the breast cancer microenvironment, we analyzed the possible regulation of PTPγ mRNA expression by KGF.
MCF-7 cells were cultured as described above and RNA was extracted after 24 hours of KGF treatment. A semi-quantitative RT-PCR analysis was performed.
As it is shown in Figure 10, KGF significantly suppresses PTPγ mRNA expression in a dose dependent manner.

Task 2: KGF peptide Three-D structural analysis

To develop small-molecules ATP-competitive inhibitors that will inhibit the kinase activity of KGFR receptor

Since KGFR is a *trans*-membrane growth factor tyrosine kinase, the design of small molecule selective inhibitors of KGFR that compete with ATP for the catalytic site represents a viable approach. As all members of the kinase family bind the same nucleotide co-factor, the dogma in the field had been that the ATP-binding cleft of this enzyme class would not prove to be a good target for drug discovery. Within the last several years a number of protein kinase selective ATP-competitive inhibitors, some of which show a high degree of selectivity, have been identified. The first ATP-competitive protein tyrosine kinase inhibitor Gleevec® (STI571) was approved last year for the treatment of chronic myelogenous leukemia (CML). No known ATP-competitive KGFR antagonists have ever been reported. In addition, unlike other protein kinases, the X-ray crystal of the receptor is not known. Fortunately the x-ray crystal structure of the other FGF family member, FGFR1 is available. The FGFR-1 tyrosine kinase domain has been crystallized and structures determined in complex with inhibitors **PD173074 (2FGI), SU4984 (1AGW), and SU5402 (1FGI)** and this protein has 86% homology to the KGFR tyrosine kinase domain. The amino acid sequence alignment of human KGFR (hKGFR), mouse KGFR (mKGFR) and FGFR-1 tyrosine kinase domains is shown below (Fig 11).

```
hKGFR: 481 LTLGKPLGEGCFGQVVMAEAVGIDKDKPKEAVTVAVKMLKDDATEKDLSDLVSEMEMMKM 540
mKGFR: 481 LTLGKPLGEGCFGQVVMAEAVGIDKDKPKEAVTVAVKMLKDDATEKDLSDLVSEMEMMKM 540
FGFR1: 478 LVLGKPLGEGAFGQVVLAEAIGLDKDKPNRVTKVAVKMLKSDATEKDLSDLISEMEMMKM 537
hKGFR: 541 IGKHKNIINLLGACTQDGPLYVIVEYASKGNLREYLRARRPPGMEYSYDINRVPEEQMTF 600
mKGFR: 541 IGKHKNIINLLGACTQDGPLYVIVEYASKGNLREYLRARRPPGMEYSYDINRVPEEQMTF 600
FGFR1: 538 IGKHKNIINLLGACTQDGPLYVIVEYASKGNLREYLQARRPPGLEYSYNPSHNPEEQLSS 597
hKGFR: 601 KDLVSCTYQLARGMEYLASQKCIHRDLAARNVLVTENNVMKIADFGLARDINNIDYYKKT 660
mKGFR: 601 KDLVSCTYQLARGMEYLASQKCIHRDLAARNVLVTENNVMKIADFGLARDINNIDYYKKT 660
FGFR1: 598 KDLVSCAYQVARGMEYLASKKCIHRDLAARNVLVTEDNVMKIADFGLARDIHHIDYYKKT 657
hKGFR: 661 TNGRLPVKWMAPEALFDRVYTHQSDVWSFGVLMWEIFTLGGSPYPGIPVEELFKLLKEGH 720
mKGFR: 661 TNGRLPVKWMAPEALFDRVYTHQSDVWSFGVLMWEIFTLGGSPYPGIPVEELFKLLKEGH 720
FGFR1: 658 TNGRLPVKWMAPEALFDRIYTHQSDVWSFGVLLWEIFTLGGSPYPGVPVEELFKLLKEGH 717
hKGFR: 721 RMDKPANCTNELYMMMRDCWHAVPSQRPTFKQLVEDLDRILTLTTNEE 768
mKGFR: 721 RMDKPTNCTNELYMMMRDCWHAVPSQRPTFKQLVEDLDRILTLTTNEE 768
FGFR1: 718 RMDKPSNCTNELYMMMRDCWHAVPSQRPTFKQLVEDLDRIVALTSNQE 765
```

Fig 11. Alignment of human KGFR (hKGFR), mouse KGFR (mKGFR) and FGFR-1 tyrosine kinase domains. Both receptors share 86% amino acid identity with human FGFR-1. Residues not shared between KGFR and FGFR-1 are in bold type. Residues unshared between the three proteins are also underlined.

Development of a homology model of the human KGFR using computational techniques. We have constructed a homology model of the KGFR tyrosine kinase domain using 2FGI as a template, which has the potential to guide the design of novel ATP site-directed ligands. *In silico* site-directed mutagenesis was used to generate acrude mode of the KGFR receptor tyrosine kinase domain.

Model Building and Refinement - All of the following techniques were conducted in Sybyl versions 6.7 orhigher (Tripos Associates, St. Louis, MO). The crystal structure of the FGFR-1 tyrosine kinase domain bound to the inhibitor PD173074 (PDB ID 2FGI) serves as the basis for the model. Amino acids Gly580 throughPro591 were missing from the structure. Loop searching in the Biopolymer module was used with N- and C-terminal anchor residues set to three. A single loop from 1BVP was identified and the conformation was copied to the corresponding FGFR-1 sequence. Mutation of the side chains of the FGFR-1 to the corresponding side chains of KGFR was performed with the "mutatemonomer" command. Tyr654 was phosphorylatedusing the "modify monomer" command. After the mutations were completed, side chains are minimized using the AMBER 4.1 force field. The resulting KGFR tyrosine kinase domain is then immersed into a box of TIP3P water. An unrestrained molecular dynamics (MD) simulation was performed at 300 K for 50,000 fs, with a Boltzmann distribution of initial velocities. An 8 Å non-bonded interaction cutoff was used, and the non-bonded pair list was updated every 25 fs. Structures were averaged over time periods in which the atoms had obtained a stable trajectory. The averaged structures were minimized to a gradient of 0.5 kcal/mol/angstrom, followed by 100 steps of deepest descent minimization. The crystal structure of FGFR-1 and KGFR homology model is shownbelow (Fig 12). This model has identified some keyresidues in the KGFR tyrosine kinase domain, which differ from those found in FGFR-1. Alanine 488 of theFGFR-1 tyrosine domain corresponds to a Cys residue within KGFR, because of the polarity difference s in these amino acids, ligands identified from virtual screening could be optimized to exploit a novel interaction. Another key difference in the tyrosine kinase domains of these proteins lies in a 12 amino acid stretch near the entrance to the ATP binding site (Asn589→Phe600 – DINRVPEEQMTF). Two residues in this segment, Asn 586 and Pro 587 of FGFR-1, correspond to an aspartic acid and an isoleucine respectively in KGFR (Fig 12). The lack of conformationally restricted proline in KGFR in that segment may result in a different secondary structure near the ATP binding site. The opportunity for interaction with other amino acids by selective ligands may emerge as the result of molecular dynamic simulations.

Fig 12. The crystal structure of FGFR-1 (PBD ID:1FGI) displayed with binding pocket amino acids (left)and SU5402. The KGFR homology model is displayed (right) with the DINRVPEEQMTF stretch at the bottom of the model.

Virtual screening of in-house libraries. Virtual screening of the combinatorial libraries is performed with FlexX within the Sybyl environment. This is a flexible docking method that uses and incremental construction algorithm to place ligands into the active site. When docking ligands in FGFR-1, bound ligands were used as a reference and the binding pocket defined by amino acids in a 6.5 Å sphere from ligand atoms. To validate the docking method, we tested its ability to reproduce the binding mode of SU5402 in 1FGI (Fig 13). To prepare the KGFR homology model for docking, all of the hydrogens were removed. In all cases ligands were docked with hydrogens present and formal charges were assigned to all atoms. Because the KGFR homology model lacked a bound ligand, the corresponding amino acids to those identified in FGFR-1 plus a 2.5 Å selection radius was used to create the receptor description file. The ranking of the generated solutions is performed using a scoring function that estimates the free binding energy of the protein-ligand complex.

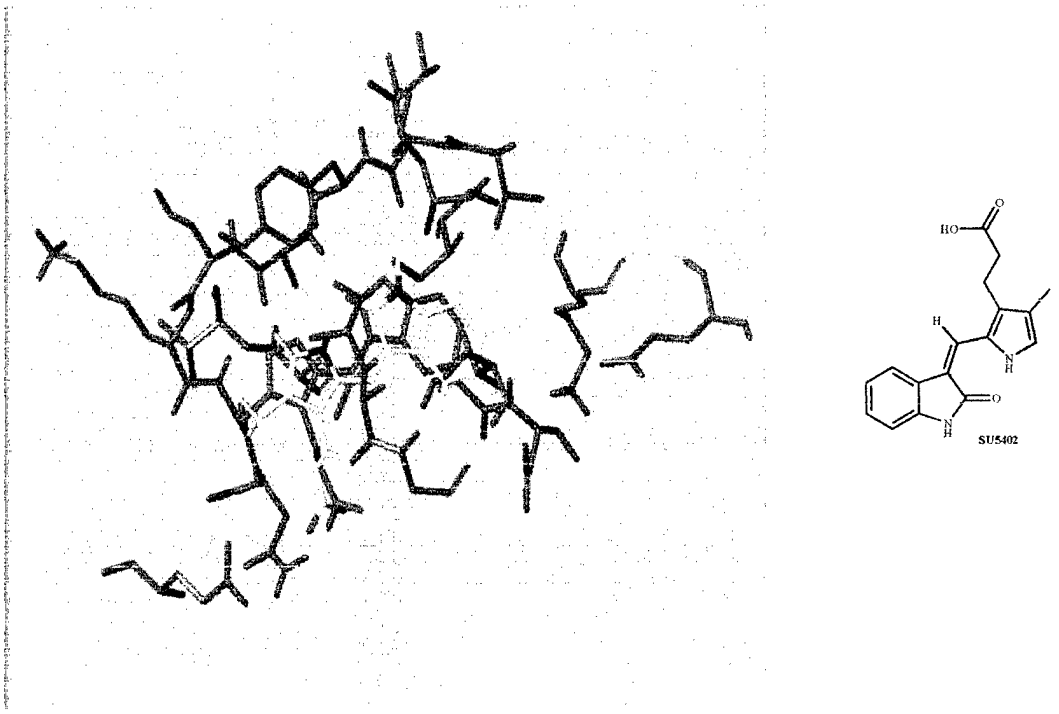

Fig 13. FlexX reproduces the binding mode of SU5402 in 1FGI with and RMS deviation of 1.08 angstroms. Protein, Reference ligand, and docked SU5402 (by atom type) are shown. Hydrogen bonds are dotted line

We have been involved in the design and synthesis protein tyrosine kinase ATP-competitive inhibitors for several years. Specifically we design inhibitors that target vascular endothelial growth factor (VEGF) and cyclin dependent kinase (CDK). Currently we have 2 series of potential inhibitors of KGFR in our in-house library. The first library contains compounds with indolinone and quinolinone structural core and their conformation ally restricted analogs (Fig. 13).

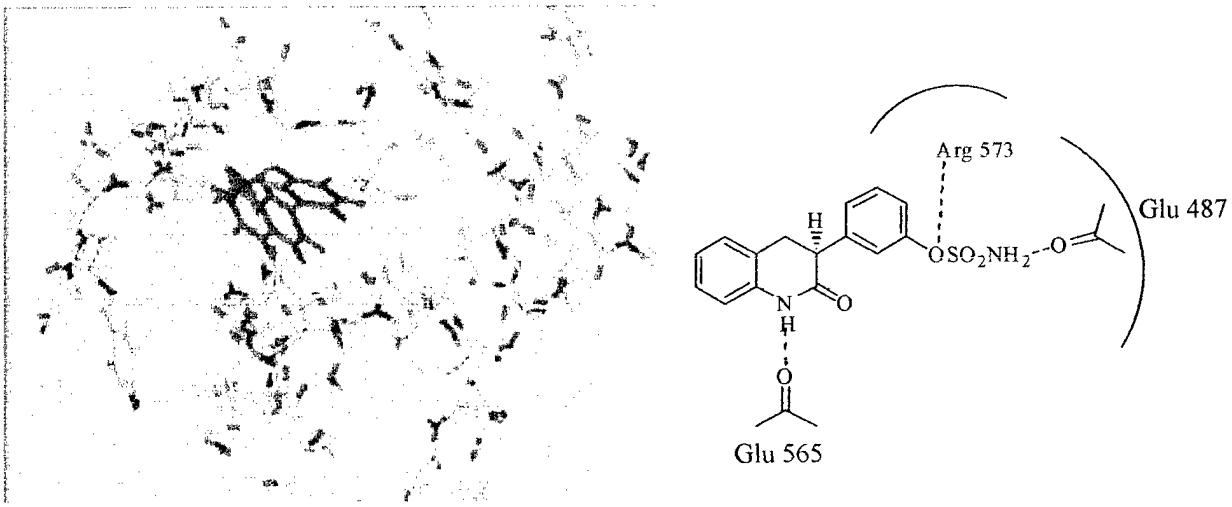

Figure 14. The binding of compound 2 to the homology model of the ATP

They are indolinone (compounds 1, 6, 8, 13-15, 21, 26, 30-31, 34-36, 51, 53 and61), dihydroquinolinones (compounds 2, 9, 16-17, 25, 45-46, 48, 57, 59, 62 and 64), quinolinones (compounds3-4, 7, 10, 12, 19-20, 22-24, 27-29, 32, 37-44, 50, 52, 55-56, 58 and 63), benzofuro (3,2-c) quinolinones (compounds 5, 47, 49 and 60) and benzofuro (2,3-b) quinolinones (compounds 11, 18, 33 and 65). Virtual screening of the library was performed with FlexX within the Sybyl environment. The ranking of the generated solutions was performed using a scoring function that estimates the free binding energy of the protein-ligand complex. The molecule with the highest estimated free binding energy is ranked 1. As expected, compound 1 (SU5402) is ranked the highest in terms of estimated binding energy. The top five compounds with the highest estimated free binding energy contain the indolinone (compound 1), dihydroquinolinone (compound 2), quinolinones (compounds 3 and 4) and benzofuro (3,2-c) quinolinones (compounds 5) structural cores. The binding of compound 2 to the homology model of the ATP pocket of KGFR is similar to SU 5402 (Fig. 14). The second series of potential inhibitors contains the benzopyranone core structures with substitutions at the 2, 3, 5, 6, 7 or 8 positions. Virtual screening of the library was performed with FlexX within the Sybyl environment. The ranking of the generated solutions was performed using a scoring function that estimates the free binding energy of the protein-ligand complex. The molecule with the highest estimated free binding energyin this series is ranked 101. Interestingly several natural products Luteolin [compound 103], Quercetin[compound 104], Hesperetin [compound 106], Morin [compound 107], chrysin [compound 109], Apigenin [compound 114] and Myricetin [compound 115] that contain the benzopyranone nucleus are ranked the highest amount the 55 compounds in the library (Fig. 16).
The binding of Quercetin to the homology model of the ATP pocket of KGFR is shown in Fig. 14. The 3'-OH and 5-OH groups of Quercetin are hydrogen bonded to the peptide backbone of Leu 487 and Lys 567 respectively. The oxygen atoms of 3-OH and 4 keto groups are hydrogen bonded to the peptide backbone of Asn 571. The oxygen atom of the 7-OH group of Quercetin serves as a hydrogen bond acceptor and bonded to Tyr 566. In addition, the hydrogen atom of the 7-OH is hydrogen bonded to the peptide backbone of Ser 568 (Fig. 17).

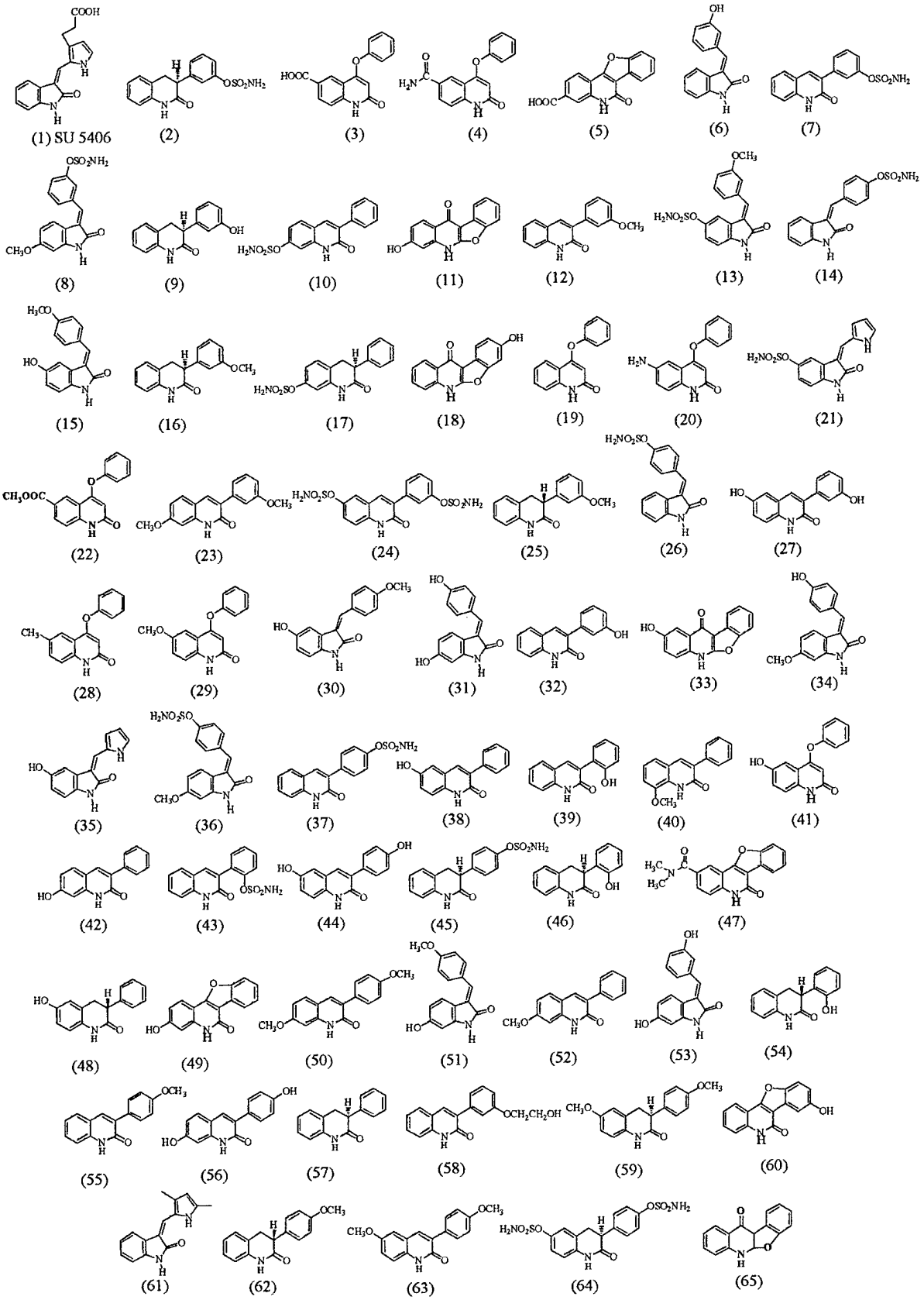

Fig. 15. Structures of indolinones, quinolinones and their conformationally restricted Analogs. The compounds are prioritized with compound having the highest free binding energy ranked compound 1 (SU5402).

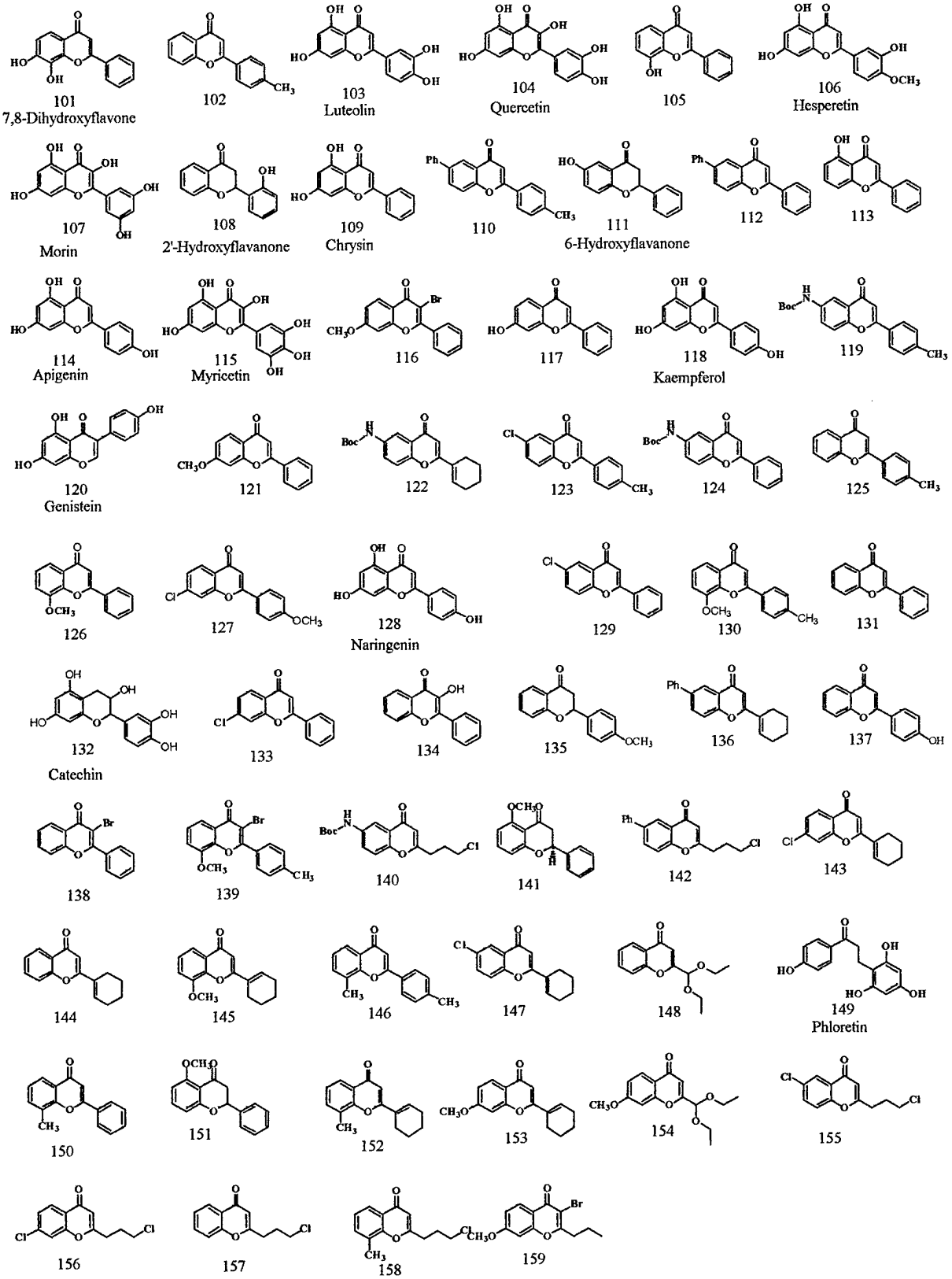

Figure 16. Structures of benzopyranone analogs

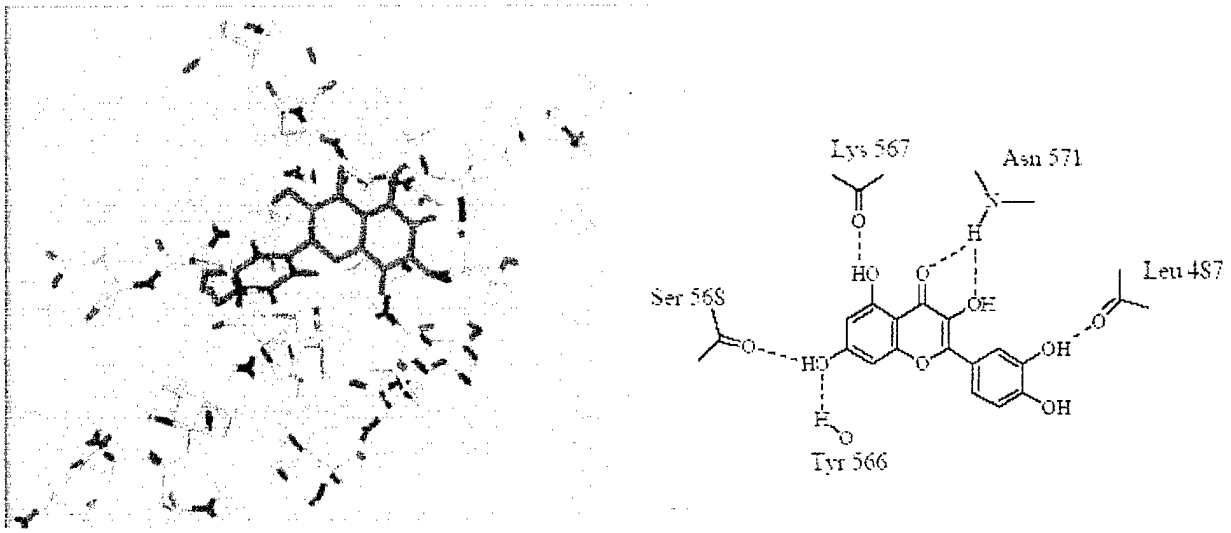

Fig 17. The binding of Quercetin to the homology model of the ATP pocket of KGFR.

The development of KGFR homology model and virtual screening of compound library is only an approach in as tructure-based directed library design. It has no meaning without the actual testing of the molecules using bioassays. The development of bioassays for the screening of the compounds is described below. The assays developed are not only used for the screening of the compounds, but also will be used for the validation of the homology model and model refinement. In the future, the inhibitory activities (IC50 values) of the compounds will be obtained and compared with the estimated free binding energy of the molecules through virtual screening to establish if there is any correlation.

Task 3: Syntheses of a series of small peptides based on 3-D structural analysis results

In order to evaluate a potency of small-molecules ATP-competitive inhibitors that would inhibit the kinase activity of KGFR receptor, we have first tested the molecules in MCF-7 cells. As it was described above, KGF down regulates ERα mRNA expression in breast cancer cells. By using real-time quantitative PCR described above, regulation of ERα mRNA by these small molecules was measured.

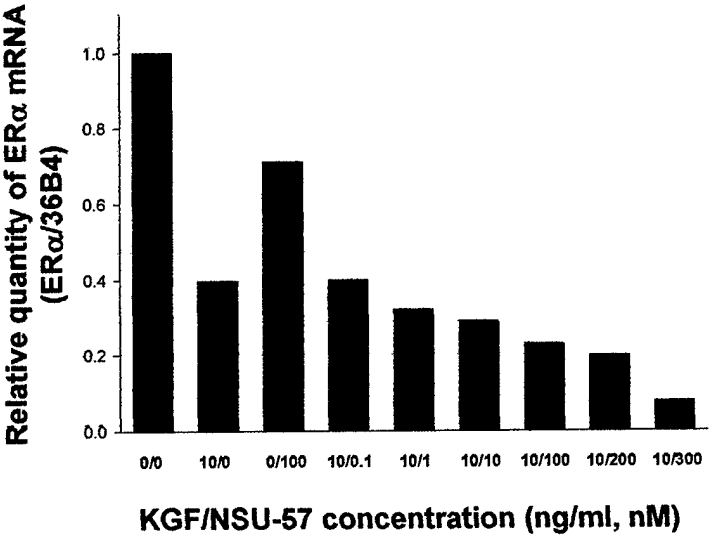

Figure 18. Effect of potential KGF inhibitor NSU-57 in MCF-7 breast cancer cell

The MCF-7 cells were cultured in phenol red-free DMEM/F12 supplemented with 0.02% bovine serum albumin for 24 hours before treatment. MCF-7 cells were treated with series of NSU compounds as shown in Figures 15 and 16, KGF or combination of the compound and KGF in phenol red-free DMEM/F12 supplemented with 5% dextran-coated charcoal treated fetal bovine serum for 24 hours. Control groups were treated with vehicle in the same medium. The mRNA expression level of ER-α in MCF-7 cells was evaluated by Real-time quantitative PCR. A detailed cell culture method were described in section 1-A. The ERα mRNA expression was suppressed by KGF in MCF-7 cells. As shown in Figure 18, compound NSU-57 alone downregulated ERα mRNA expression by 30%. The results from combination of KGF and NSU-57 treatment revealed that NSU-57 further downregulates the KGF suppressed ERα mRNA expression in dose dependent manner. We can not conclude this result without obtaining other function assay such as KGFR autophosphorilation status analysis. Although we have not completed the

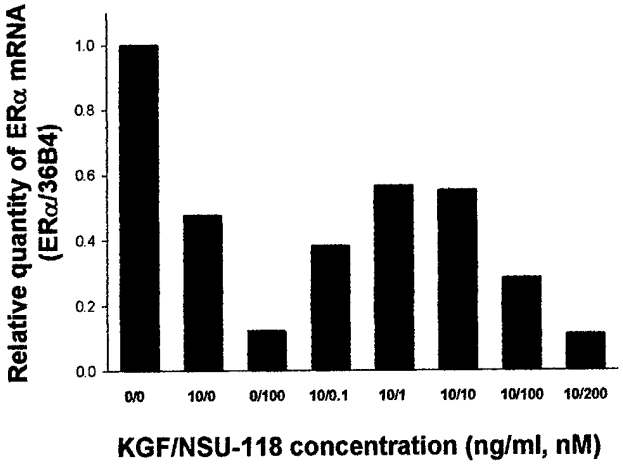

Figure 19. Effect of potential KGF inhibitor in MCF-7 breast cancer cell

development of this assay system, we have obtained some preliminary data as described in the following section. We are also on a way to develop an ELISA technique to analyze the KGFR autophosphorilation status in a 96-well format.

Figure 19 shows a similar pattern of effect of NSU compound on ERα mRNA expression in MCF-7 cells.

We have not completed the screening of all molecules listed in Figures 15 and 16, yet. The data we have obtained to date are either likes of shown in Figures 18 and 19, or no effect at all. This section of experiments is in progress.

Task 4: Syntheses of a series of modified small peptides (Months 18-20)
The first molecule that has identified as a potential responsive element to bind to KGFR, (**ArgThrValAlaVal**), was synthesized, *pep*KGF-13, and its biological activity was tested. The *pep*KGF-13 lies between residues101-105. The location and sequence of the *pep*KGF-13 is shown in red in Table 1 above.

The MCF-7 cells were cultured in phenol red-free DMEM/F12 supplemented with 0.02% bovine serum albumin for 24 hours before treatment. MCF-7 cells were treated with 5 amino acid peptide (*pep*KGF-13), KGF or *pep*KGF-13 with 10 ng/ml KGF in phenol red-free DMEM/F12 supplemented with 5% dextran-coated charcoal treated fetal bovine serum for 24 hours. Controls were treated with vehicle in the same medium. The mRNA expression level of ER-α in MCF-7 cells was evaluated by Real-time quantitative PCR. A detailed cell culture methods were described in section 1-A.
KGF treatment of MCF 7 cells suppressed ER-α mRNA expression in a dose dependent manner. Both KGF and high concentration of *pep*KGF-13 suppressed ER-α mRNA expression levels by 35- 50%. KGF plus *pep*KGF-13 further reduced ER-α mRNA level by 65%. Our results indicated that KGF downregulates ER-α mRNA expression in MCF-7 cells. A five amino acid sequence of KGF at high concentration worked as an agonist to facilitate the suppression of ER-α mRNA expression. In addition, *pep*KGF-13 failed to suppress the KGF suppressed ER-α mRNA expression.
It should be, however, noted that at low concentrations, *pep*KGF-13 was not as effective as it worked at a high concentration. We are currently unable to explain this inconsistency of *pep*KGF-13 on ERα mRNA expressions in breast cancer cell line MCF-7. Similar inconsistency was also observed in a DNA synthesis assay system. In order to explain this inconsistency, we have performed a solid phase binding study as described above. However the result reviled that the *pep*KGF-13 did not bind to KGFR overexpressed extracellular domain. This may be due to lack of other molecules in the assay system (*e.g.* lack of heparin). Further studies are needed to clarify this hypothesis. We believe that this is at least a partial reason to explain the inconsistency of the *pep*KGF-13 effects in MCF-7 cells. This part of studies is still in progress.

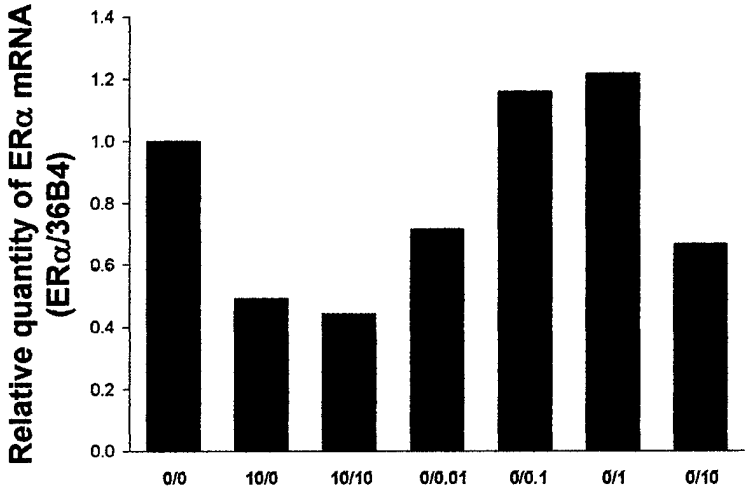

Figure 20. Effect of potential KGF antagonist *pep*KGF-13 in MCF-7 breast cancer cell

It is also important to mention that we have analyzed the progesterone receptor (PR) mRNA expression by a real-time quantitative PCR. PR is a well known molecule which

is upregulated by estrogen thorough estrogen receptor pathway. Therefore, we believe that the *pep*KGF-13 did not interact with estrogen receptor.

Cellular Kinase assay development: A high-throughput, 96 well format ELISA will be established to screen for inhibitors of KGFR kinase activity. As shown in Figure 21, KGFR autophosphorilation (120kDa band) is detectable by an immunoprecipitation analysis. This should be noted that the strong band appeared at 60kDa in the Figure 21 was a nonspecific band which is a part of heavy chain of IgG that are said to be cleaved by 2-mercapt ethanol. A 20 minute of 20ng/ml KGF treatment induces phosphorylation of KGFR in A549, non-small lung cancer cell line that is known as a KGFR overexpress cells. The same antibodies set (our KGFR specific antibody described above; Anti-Phosphotyrosine, Clone 4G10, Upstate) used this experiment will be utilized for the following cellular kinase assay. NIH 3T3 cells expressing KGFR will be stimulated with KGF, and lysates of the cells will be subjected to a sandwich ELISA with antibodies against KGFR and phosphotyrosine. Briefly, NIH 3T3-KGFR cells will be plated onto 96-well plates in 10% FBS/DMEM and cultured overnight, followed by serum depletion in 0.1 % FBS/DMEM for 24 h. Serial dilution of compounds will be added and the cells will be incubated for 1 h. Phosphorylation will be stimulated by the addition of human recombinant KGF (PeproTech, Inc., Rocky Hill, NJ). After incubation at 37oC, cells will be washed with PBS and lysed. Lysates will be transferred to 96 well plates precoated with polyclonal anti-KGFR antibody and incubated. Phosphotyrosine will be detected by a monoclonal anti-phosphotyrosine antibody and peroxidase-conjugated anti-mouse IgG. IC50 values of the inhibitors will be determined.

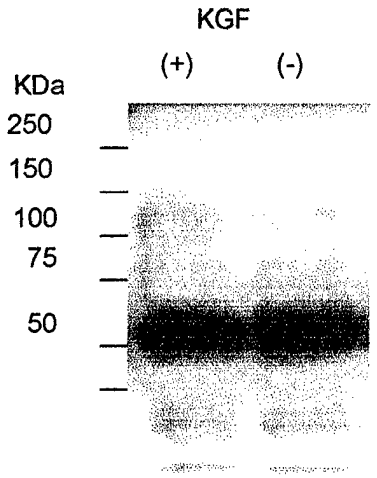

Figure 21. Induction of autophospholirated KGFR by KGF in the A549 human lung cancer cell line

As described above, the assay required a cell line over-expressed KGFR. In order to eliminate potential effects of endogenous KGFR in the breast cancer cell lines, we will initially use the NIH-3T3, a mouse fibroblast cell line. We have generated a sub-cell line of NIH-3T3 over-express KGFR through transfection. The plasmid λpCEV27-KGFR, mouse KGFR cDNA cloned in a mammalian expression vector □pCEV27, was obtained from Dr. Toru Miki, NCI (Bethesda, MD) and the NIH-3T3 cell was stably transfected with this plasmid. The cells were selected by using G-418 antibiotics and highly expressed cells with KGFR were further cultured and propagated for the further studies. The selected cells showed a response to the KGF treatment *in vitro* (75% cell proliferation induction after 24hrs KGF treatment at 2ng/ml).
This assay system will be utilized to screen the compounds listed in Figures 16 and 17.

Key Research Accomplishments

1. Based on the finding through this funded proposal we propose the estrogen and KGF involvement of human breast microenvironment as drawn in the scheme below.

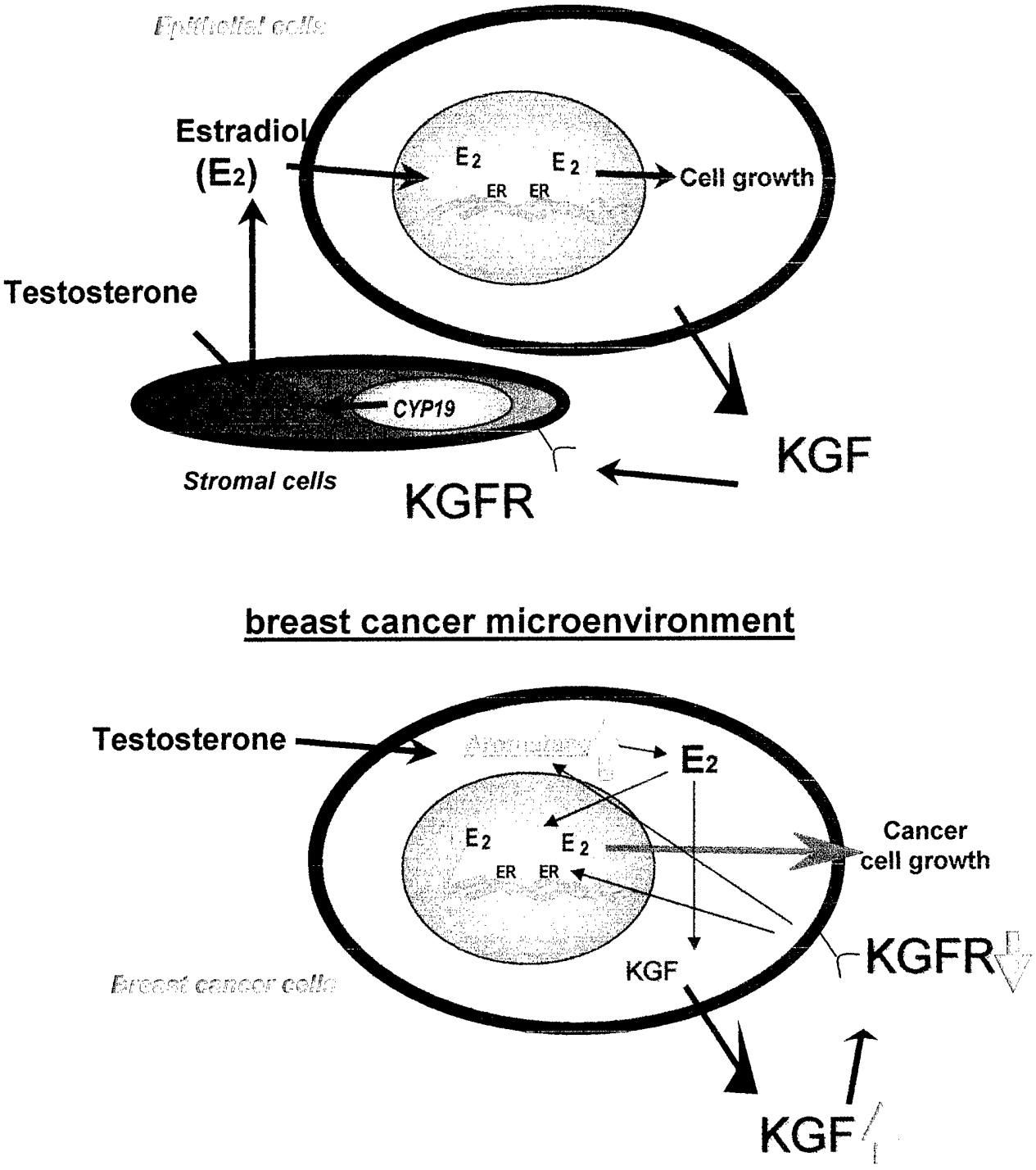

Figure 22. Proposed breast microenvironment

Reportable outcomes

A KGFR specific polyclonal antibody was generated and utilized for an immunohistochemincal analysis. To date this is the most specific KGFR antibody available. We have also showed that this antibody can be utilized for an immuno precipitation analysis and a KGFR autophosphorilation specific ELISA.

We proposed that ERα involvement in KGF-estrogen positive feed back system in breast microenvironment. This is an addition to our previously proposed mechanism.

Extensive intracellular KGFR inhibitor *in silico* analyses was performed and the small molecules were screened for possible functional inhibitor to KGFR.

Conclusions

We added a new dimension to an estrogen-KGF involved human breast microenvironment (*i.e.* KGF regulates estrogen receptor α mRNA and protein expression). This part of outcome is in a manuscript we are planning to submit, soon (Chang and Sugimoto)

Although we were unable to show an effective synthetic peptide antagonist to KGF in breast cells, we developed many assay system and tools that can be used for further studies.

Referrences

Liu S, Sugimoto Y, Sorio C, Tecchio C, Lin YC. Functional analysis of estrogenically regulated protein tyrosine phosphatase γ (PTPγ) in human breast cancer cell line MCF-7. Oncogene, 23:1256-1262, 2004.

Kashida Y, Sugimoto Y, Liu SL, Lin YC. Protein tyrosine phosphatase gamma (PTP gamma) mRNA expressions in the non-tumorous or tumorous uterus tissue. BIOLOGY OF REPRODUCTION 68: 167 Suppl. 1 2003

Park KY, Sugimoto Y, Liu SL, Chang HL, Ye WP, Wang LS, Lin YC,Involvement of breast adiopocytes on local estrogen level. BIOLOGY OF REPRODUCTION 68: 444 Suppl. 1 2003

Jiang JH, Kulp SK, Sugimoto Y, Liu SL, Chang HL, Lin YC, Effects of estrogens and age on the growth of canine prostatic cells. BIOLOGY OF REPRODUCTION 68: 176 Suppl. 1 2003

Chang HL, Sugimoto Y, Park KY, Liu SL, Ye WP, Wang LS, Huang YW, Lin YC, Regulation of estrogen receptor-alpha mRNA expression by keratinocyte growth factor (KGF) in MCF-7 cells. BIOLOGY OF REPRODUCTION 68: 659 Suppl. 1 2003

Liu SL, Sugimoto Y, Kulp SK, Jiang JH, Chang HL, Park KY, Kashida Y, Lin YC Estrogenic down-regulation of protein tyrosine phosphatase gamma (PTP gamma) in human breast is associated with estrogen receptor alpha ANTICANCER RESEARCH 22 (6C): 3917-3923

Jiang JH, Ghosh PK, Kulp GK, Sugimoto Y, Liu SL, Czekajewski J, Chang HL, Lin YC Effects of gossypol on O-2 consumption and CO2 production in human prostate cancer cells ANTICANCER RESEARCH 22 (3): 1491-1496

Chang HL, Sugimoto Y, Liu SL, Jiang JH, Kulp SK, Park KY, Kashida Y, Lin YC Regulation of protein tyrosine phosphatase gamma (PTP gamma) mRNA expression by estrogenically active agents in canine prostate. BIOLOGY OF REPRODUCTION 66: 591 Suppl. 1 2002

Appendices

Liu S, Sugimoto Y, Sorio C, Tecchio C, Lin YC. Functional analysis of estrogenically regulated protein tyrosine phosphatase γ (PTPγ) in human breast cancer cell line MCF-7. Oncogene, 23:1256-1262, 2004.

Oncogene (2004) 23, 1256–1262

www.nature.com/onc

Function analysis of estrogenically regulated protein tyrosine phosphatase γ (PTPγ) in human breast cancer cell line MCF-7

Suling Liu[1], Yasuro Sugimoto[1,2], Claudio Sorio[3], Cristina Tecchio[3] and Young C Lin*[,1,2]

[1]*Laboratory of Reproductive and Molecular Endocrinology, College of Veterinary Medicine, The Ohio State University, Columbus, OH 43210, USA;* [2]*The Ohio State University Comprehensive Cancer Center; The Ohio State University, Columbus, OH 43210, USA;* [3]*Dipartimento di Patologia, Universita di Verona, Strada le Grazie 37134, Verona, Italy*

Protein tyrosine phosphatase γ (PTPγ) is a member of the receptor-like family of tyrosine phosphatases and has been implicated as a tumor suppressor gene in kidney and lung cancers. Based on our previous findings, we hypothesize that PTPγ is a potential estrogen-regulated tumor suppressor gene in human breast cancer. To examine the effects of PTPγ on growth of MCF-7 human breast cancer cells and compare the estrogenic responses of human breast cells with different PTPγ expression levels, we established several stably transfected MCF-7 cell lines expressing different levels of PTPγ, which were confirmed by RT–PCR and immunostaining. In our work, we used the antisense construct to breakdown endogenous PTPγ level in MCF-7 cells. The results from doubling time assay suggested that PTPγ is capable of inhibiting MCF-7 breast cancer cell growth. We further demonstrated that PTPγ is able to inhibit anchorage-independent growth of breast cancer cells in soft agar and reduce the estrogenic responses of MCF-7 cell proliferation to estradiol-17β (E_2) and zeranol (Z, a nonsteroidal growth promoter with estrogenic activity). Our data suggest that PTPγ may function as an important modulator in regulating the process of tumorigenesis in human breast.
Oncogene (2004) **23,** 1256–1262. doi:10.1038/sj.onc.1207235
Published online 15 December 2003

Keywords: human breast; human breast cancer; protein tyrosine phosphatase γ; overexpression; antisense; soft agar assay

Introduction

Protein tyrosine phosphatases (PTPases) are a family of proteins that perform the enzymatic role to remove phosphate groups from phosphotyrosine residues of specific targets inside cells. PTPases regulate important cellular processes like gene expression, cell activation and proliferation, differentiation, development, transport and locomotion, since they counterbalance the growth-promoting effects of protein tyrosine kinases (PTKs), which catalyse the phosphorylation of tyrosine residues (Shock *et al.*, 1995). Therefore, alterations in PTPs activity might affect cell growth, neoplastic processes and transformation (Gaits *et al.*, 1995). Addition of the PTPase-inhibitor vanadate to cells in culture leads to increased amounts of phosphotyrosine-containing proteins and cellular transformation (Klarlund, 1985). Therefore, a delicate balance between PTK and PTPase action is essential for normal functioning of cells.

PTPγ is a member of the receptor-like family of tyrosine-specific phosphatases originally cloned from human brainstem and placental cDNA libraries using probes derived from the intracellular domain of CD45 (Kaplan *et al.*, 1990) or *Drosophila* PTPase cDNA clone, DPTP12 (Krueger *et al.*, 1990), respectively. The structure of the receptor-like PTPs (RPTPs) includes an extracellular, a transmembrane, and one or two tandemly repeated catalytic domains. This structure implies a ligand-binding capability that may modulate enzymatic activity. However, the putative ligands for most of the PTPs with receptor-like structures are yet to be identified. Receptor-like PTPγ has a carbonic anhydrase-homologous amino terminus followed by a fibronectin type three domain, a cysteine-free domain, a transmembrane domain and two intracellular PTPase catalytic domains (Krueger and Saito, 1992; Barnea *et al.*, 1993; Levy *et al.*, 1993). According to mRNA analysis (LaForgia *et al.*, 1991; Barnea *et al.*, 1993), PTPγ is a broadly expressed enzyme that exists in many tissues, including human lung, stomach, esophagus, colon, liver, spleen and kidney (Tsukamoto *et al.*, 1992). Based on the chromosomal location of the PTPγ gene (3p14.2) (LaForgia *et al.*, 1991, 1993) and studies showing loss of heterozygosity of the gene in kidney tumors (Lubinski *et al.*, 1994), PTPγ has been implicated as a candidate tumor suppressor gene. More recently, PTPγ expression levels were shown to be reduced in ovarian and lung tumors (van Niekerk and Poels, 1999). Our previous results showed lower PTPγ mRNA expression levels in diethylstilbestrol-induced kidney tumors in hamsters than in normal hamster kidney (Lin *et al.*, 1994). Also, we have shown that, in ACI rats,

*Correspondence: YC Lin, Laboratory of Reproductive and Molecular Endocrinology, College of Veterinary Medicine, The Ohio State University, 1900 Coffey Road, Columbus, OH 43210-1092, USA;
E-mail: lin.15@osu.edu
Received 25 June 2003; revised 22 September 2003; accepted 22 September 2003

PTPγ is localized to the mammary epithelium and that zeranol (Z), a nonsteroidal agent with estrogenic activity that is used as a growth promoter in the US beef and veal industries, can suppress PTPγ mRNA levels in mammary glands (Kulp *et al*., 2000). Furthermore, we have reported that PTPγ is expressed in normal and malignant human breast epithelium, and PTPγ mRNA levels can be suppressed by estrogens through an estrogen receptor-mediated mechanism (Zheng *et al*., 2000). More recently, our results showed that PTPγ mRNA expression was lower in cancerous than in normal breast tissues; both 17β-estradiol (E_2) and Z suppressed PTPγ mRNA levels in both cultured normal breast tissues and cultured breast cells isolated from normal breast tissues. In whole breast tissues, PTPγ was immunolocalized to the epithelium and treatment with E_2 or Z diminished PTPγ staining, which indicated reductions in PTPγ at the protein level (Liu *et al*., 2002). These findings suggest that PTPγ is a potential estrogen-regulated tumor suppressor gene in human breast cancer that may play an important role in neoplastic processes of human breast epithelium, and indicate an intriguing relationship among cancer, estrogen and PTPγ.

The aim of the present study was to examine the effect of PTPγ on the growth of human breast cancer and compare the estrogenic responses of human breast cells with different expression levels of PTPγ. MCF-7 breast cancer cells were used as a model and we stably transfected a plasmid containing the whole PTPγ coding sequence or containing a small portion of PTPγ coding sequence in the antisense orientation into human MCF-7 breast carcinoma cells. PTPγ-overexpressing MCF-7 cells normally show the characteristics with slow-growing and lower colony efficiency on soft agar, and show antiestrogenic effects on human breast cell proliferation.

Results

Comparison of PTPγ expression in stably transfected MCF-7 cells

MCF-7 cells were transfected with pCR®3.1 vector (M7-pCR®3.1–800 (s)), full-length PTPγ (M7-PTPγ-800 (s)), PTPγ antisense construct (M7-A24-800 (s)) or PTPγ sense construct (M7-B19-800 (s)). Based on the dose–response curve of each transfected cell line to G-418, it was determined that 800 μg/ml was the optimal dose of G-418 for the single colony selection in every transfected cell line. We have selected five single clones from mock-transfected MCF-7 cells (M7-pCR®3.1-800 (s)), 19 single clones from PTPγ-transfected MCF-7 cells (M7-PTPγ-800 (s)), 17 single clones from antisense PTPγ-transfected MCF-7 cells (M7-A24-800 (s)) and 11 single clones from sense PTPγ-transfected MCF-7 cells (M7-B19-800 (s)). To identify the successfully and ideally transfected single colonies, RT–PCR with a set of specific primers was used for each group of transfection (Figure 1). The results showed that 13 out of 19 clones from M7-PTPγ-800 (s) expressed exogenous PTPγ mRNA, and all of the single clones from M7-pCR®3.1-800, M7-A24-800 and M7-B19-800 were successful. Furthermore, PTPγ mRNA expression was compared among those successfully transfected cell lines. Our results showed that M7-PTPγ-800 (s) had higher PTPγ mRNA expression than any of wild-type MCF-7, M7-pCR®3.1–800, M7-A24-800 and M7-B19-800 cell lines. M7-A24-800 had lower PTPγ mRNA expression than any of wild-type MCF-7, M7-pCR®3.1-800, M7-PTPγ-800 and M7-B19-800 cell lines (Figure 2). Also, the results from immunohistochemical staining showed that the PTPγ staining was weak and very similar to that of wild-type MCF-7 cell (Figure 3a), M7-pCR®3.1-800 (s) (Figure 3b) and M7-B19-800 (s) (Figure 3c). Furthermore, the degree of staining was observably increased in M7-PTPγ-800 (s) (Figure 3d) when compared to others; however, the degree of staining was almost diminished in M7-A24-800 (s) (Figure 3e) when compared to others. Thus, these results indicate that PTPγ is overexpressed in M7-PTPγ-800 (s) and is greatly reduced in M7-A24-800 (s) compared to other cells. These results are consistent with those presented in Figure 2.

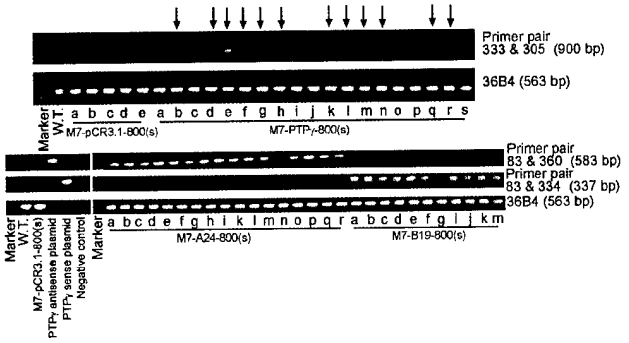

Figure 1 Identification and confirmation of successfully transfected cell lines by RT–PCR. A total of 1.5×10^5 viable cells from wild-type MCF-7 cells and each single colony were plated in one well of six-well plates with 5 ml of culture medium separately and cultured to ~85% confluence, total RNA was isolated for each group, and RT–PCR was performed. Ethidium bromide-stained PCR products separated in a 1.5% agarose gel. 36B4 was used as internal standard. Primer 305 is located in BGH reverse priming site in pCR®3.1 vector; primer 333 is located in the sense strand of full-length PTPγ cDNA insert; primer 83 is located in T7 promoter/priming site in pCR®3.1 vector; primer 360 is located in the antisense strand of the partial PTPγ cDNA insert; primer 334 (complementary to primer 360) is located in the sense strand of the partial PTPγ cDNA insert. W.T.: wild-type MCF-7 cells

Effects of PTPγ on the proliferation of MCF-7 cells

To check whether PTPγ level has an antimitogenic effect on MCF-7 cells, a proliferation study was performed by means of doubling time assay. Wild-type MCF-7 cells, M7-pCR®3.1-800 (s) and M7-B19-800 (s) had the mean cell population doubling time of 24.0 ± 2, 24.3 ± 3 and 23.8 ± 1 h, respectively, but it was increased to 40.0 ± 3 h for M7-PTPγ-800 (s) (~60% increase) and it was decreased to 16.4 ± 1 h for M7-A24-800 (s) (~34% decrease) (Figure 4). These results suggested that PTPγ

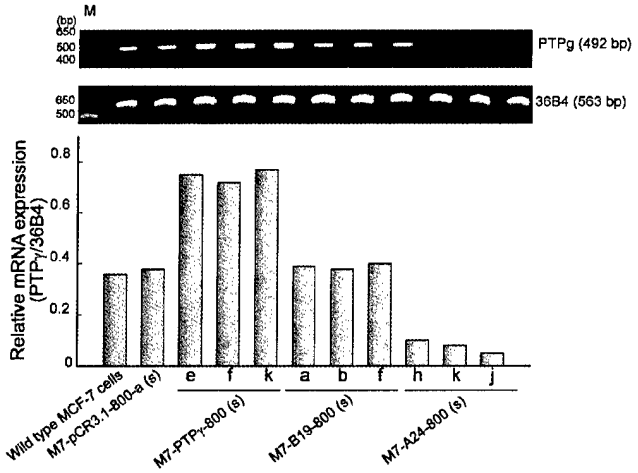

Figure 2 Expression of PTPγ mRNA in transfected MCF-7 cells. A total of 1.5×10^5 viable cells from wild-type MCF-7 cells, one of single colonies from mock transfected MCF-7 cells, and three of single colonies from M7-PTPγ-800 (s), M7-B19-800 (s) or M7-A24-800 (s) were plated in one well of six-well plates with 5 ml of culture medium separately and cultured to ~85% confluence, total RNA was isolated for each group, and RT–PCR was performed. *Top*: Ethidium bromide-stained PCR products separated in a 1.5% agarose gel. Cells were not treated and total RNA was isolated from each cell type separately. 36B4 was used as internal standard. *Bottom*: The mRNA ratios of PTPγ to 36B4 as measured by densitometry

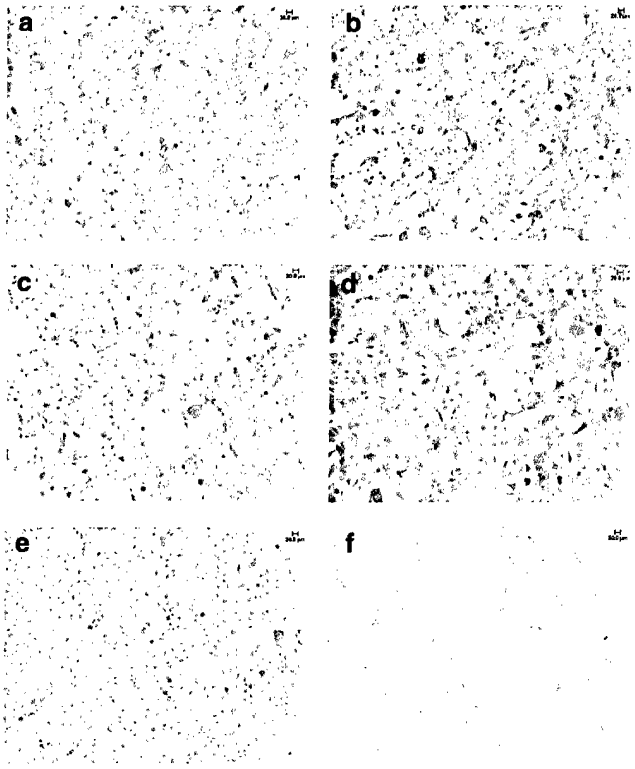

Figure 3 Immunohistochemical staining for PTPγ in transfected MCF-7 cells. Cells were cultured on 24 × 30 mm cell culture cover slips overnight and washed in PBS for three times. After −10°C methanol fixation for 5 min and air-dry, cells were stained for PTPγ by using VECTASTAIN® Universal Quick Kit and DAB Substrate Kit. Brown staining represents PTPγ immunoreactivity; blue staining represents nuclei: (**a**) Wild-type MCF-7 cells; (**b**) M7-pCR®3.1-800 (s); (**c**) M7-B19-800 (s); (**d**) M7-PTPγ-800 (s); (**e**) M7-A24-800 (s); (**f**) negative control

can inhibit MCF-7 breast cancer cell growth and plays an important role in tumor suppression of breast cancer.

Effects of PTPγ on anchorage-independent growth of MCF-7 cells

The acquisition of anchorage-independent growth is generally considered to be one of the *in vitro* properties associated with the malignancy of cells. The transfected cells were examined for their ability to grow in soft agar. First, we checked the optimal number of cells for the colony formation in six-well plates seeded with different number of wild-type MCF-7 cells, M7-pCR®3.1-800 (s) or M7-PTPγ-800 (s). The results showed that the colony number in soft agar was increased while the seeded cell number was increased for each cell type, M7-PTPγ-800 (s) formed much less and smaller colonies in soft agar than wild-type MCF-7 cells and M7- pCR®3.1-800 (s) in the same seeded cell number group (data not shown). Also, we determined that 8000 cells/well was the optimal MCF-7 cell number for the future soft agar assay in our experiment. Furthermore, we found that M7-PTPγ-800 (s) formed less and smaller colonies in soft agar than wild-type MCF-7 cells and M7- pCR®3.1-800 (s), but M7-A24-800 (s) formed more and much larger colonies in soft agar than wild-type MCF-7 cells, M7- pCR®3.1-800 (s) and M7-B19-800 (s) (Figure 5). These *in vitro* data indicated that PTPγ is able to inhibit proliferation and anchorage-independent growth of breast cancer cells.

Effects of PTPγ on estrogenic activities of E_2 and Z on MCF-7 cell proliferation

As we have known, E_2 is a potent mitogen for human breast cancers. Z is a nonsteroidal anabolic growth promoter with estrogenic activities. Our previous results showed that both Z and E_2 could induce normal human breast epithelial cell transformation and stimulate human breast cell proliferation in a dose-dependent manner, and suggested that PTPγ is a potential estrogen-regulated tumor suppressor gene in human breast cancer that may play an important role in neoplastic processes of human breast epithelium, which indicates an intriguing relationship among cancer, estrogen and PTPγ. The established stably transfected cell lines with different PTPγ expression levels were used to examine whether PTPγ has any antiestrogenic activities on MCF-7 cell proliferation. Our results showed that both Z and E_2 could stimulate the cell proliferation of wild-type MCF-7, M7-pCR®3.1-800 (s), M7-PTPγ-800 (s), M7-B19-800 (s) and M7-A24-800 (s) in a dose-dependent manner, and the potency of Z and E_2 are very similar on the stimulation of cell proliferation (Figure 6). Most interestingly, the degree of Z's or E_2's stimulation on M7-PTPγ-800 (s) cell proliferation

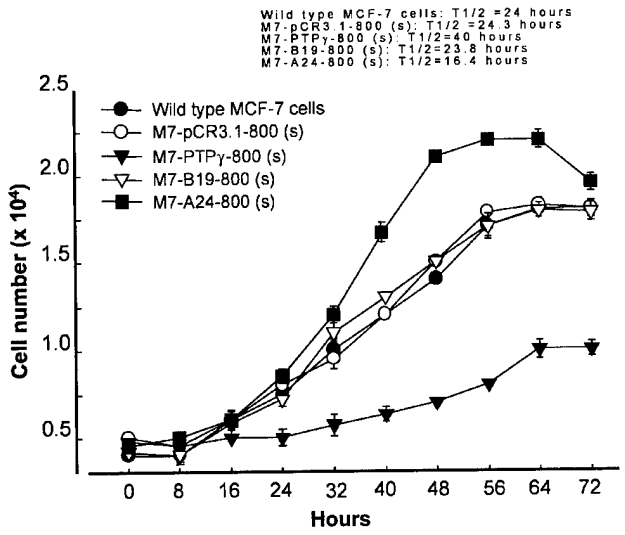

Figure 4 Effects of PTPγ on the proliferation of MCF-7 cells. In total, 5000 cells/well were seeded in 24-well plates and cells were grown for 3 days and counted every 8 h. Experiments were performed in four replicate wells, and each experiment was repeated twice. Cell doubling (CD) was calculated by using the formula: $\ln(N_j - N_i)/\ln 2$, where N_j or N_i is the cell numbers at different time point T_j or T_i ($T_j > T_i$) in the growth log phase of the cells. DT was consequently obtained by dividing the time interval ($T_j > T_i$) by CD

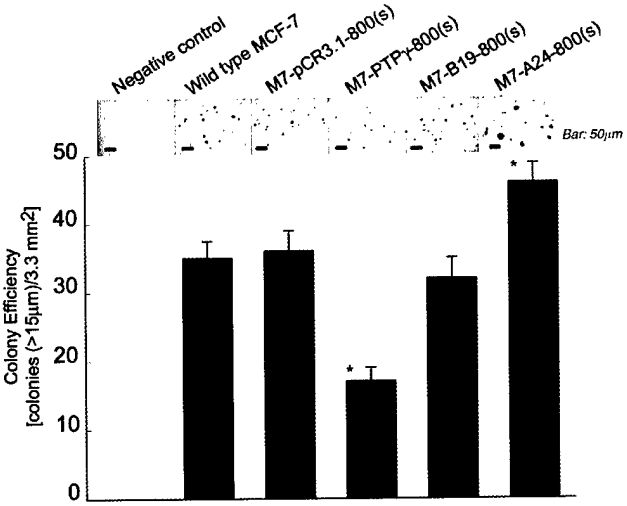

Figure 5 Effects of PTPγ on anchorage-independent growth of MCF-7 cells. (**a**) Colony formation of different MCF-7 cell types in soft agar. Cells were cultured in six-well plates first covered with an agar layer (phenol red-free high-calcium DMEM/F12 with 0.5% agar and 10% FBS). The middle layer contained 8000 cells/well in phenol red-free DMEM/F12 with 0.35% agar and 10% FBS. The top layer, consisting of medium, was added to prevent drying of the agar in the plates. The plates were incubated for 21 days, after which the plates were stained in 0.5 ml of 0.005% crystal violet for >1 h and the cultures were inspected and photographed. (**b**) Comparison of CE among different MCF-7 cell types. CE was determined by a count of the number of colonies greater than 15 μm in diameter, which was calculated as the average of colonies counted at ×50 magnification in five individual fields by using BioQuant NOVA software. Bar: 50 μm

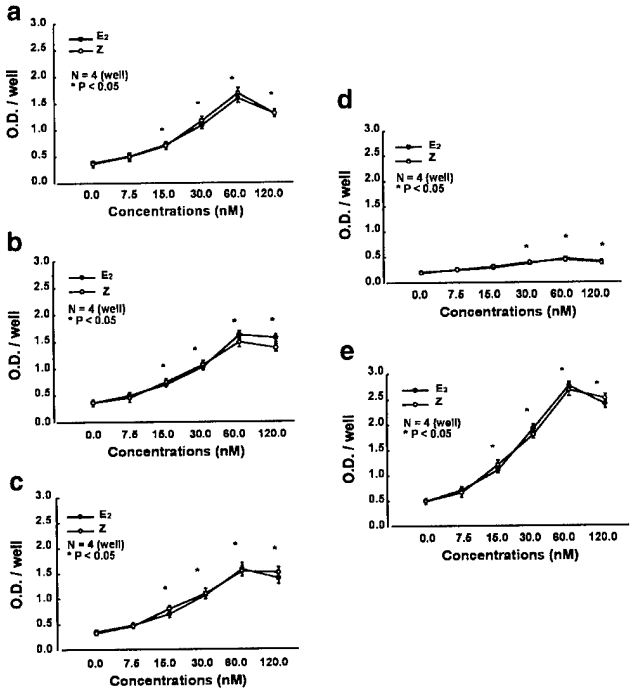

Figure 6 Effects of PTPγ on estrogenic activities of E_2 and Z on MCF-7 cell proliferation. In total, 2×10^4 cells were cultured in each well of 24-well plates and treated with the E_2 or Z at 0, 7.5, 15, 30, 60 or 120 nM in phenol red-free high-calcium DMEM/F12 supplemented with DCC-stripped FBS (5%) for 24 h. Cell proliferation rate was quantified by using CellTiter 96™ AQueous assay and optical density was read at 490 nm ($OD_{490\,nm}$) in 96-well plates by an ELISA plate reader. Each point presented the mean ± s.d. of four replicate culture wells. Asterisk represents the significant difference from the control group. A probability (P) of less than 0.05 was considered to be statistically significant ($P < 0.05$). (**a**) Wild-type MCF-7 cells; (**b**) M7-pCR®3.1-800 (s); (**c**) M7-B19-800 (s); (**d**) M7-PTPγ-800 (s); (**e**) M7-A24-800 (s)

(Figure 6d) is much less than that on the cell proliferation of wild-type MCF-7, M7-pCR®3.1-800 (s) or M7-B19-800 (s) cell proliferation (Figure 6a–c); however, the degree of Z's or E_2's stimulation on M7-A24-800 (s) cell proliferation (Figure 6e) is much greater than that on the cell proliferation of wild-type MCF-7, M7-pCR®3.1-800 (s) or M7-B19-800 (s) cell proliferation (Figure 6a–c). These results indicated that PTPγ overexpression could reduce the estrogenic responses of MCF-7 cell proliferation to E_2 and Z and has antiestrogenic activities on human breast cancer cells.

Discussion

Transmembrane receptor tyrosine phosphatases represent a growing family of enzymes, the structural features of which suggest a role in the control of cellular phosphotyrosine balance. However, the biological significance of PTPγ is only poorly understood. PTPγ has been considered as a candidate tumor suppressor gene due to the location of its gene on human chromosome 3p14.2, in a region found to be frequently deleted in

certain types of renal and lung carcinoma (LaForgia *et al*., 1991, 1993; Barnea *et al*., 1993). Our previous results suggest that PTPγ is a potential estrogen-regulated tumor suppressor gene in human breast cancer that may play an important role in breast tumorigenesis (Lin *et al*., 1994; Kulp *et al*., 2000; Zheng *et al*., 2000; Liu *et al*., 2002). But, the function of PTPγ in human breast cancer is still not clear.

To examine the effect of PTPγ on the growth properties of human breast cancer cells *in vitro* and provide a biochemical background for understanding PTPγ function, we transfected PTPγ-expressing vector with a variant full-length PTPγ cDNA lacking the intracellular juxtamembrane exon of the reported PTPγ cDNA, which is expressed as the dominant isoform in most tissues (Sorio *et al*., 1995), or PTPγ antisense construct into MCF-7 cells. It is clear from the data shown in Figure 4 that the relationship of link for the PTPγ and longer doubling time as well as less colony formation is intimately related. When the breast cancer cells have higher levels of PTPγ mRNA or its protein, the proliferative ability of breast cancer cells will be greatly suppressed or blocked.

The results from doubling time assay and soft agar assay showed that MCF-7 cells overexpressing PTPγ has the characteristics with slow-growing and lower colony efficiency on soft agar. Furthermore, the results from the cell proliferation assay showed that MCF-7 cells overexpressing PTPγ can antagonize estrogenic effects of E_2 and Z on MCF-7 cell proliferation, which indicates PTPγ has antiestrogenic effects on human breast cancer.

In combination with our previous results which showed that PTPγ mRNA expression was significantly lower in cancerous than in normal breast tissues and both E_2 and Z suppressed PTPγ mRNA levels in cultured normal breast tissues and cultured normal breast cells isolated from the tissues, all these experimental data support our suggested concept that PTPγ is a potential estrogen-regulated breast cancer suppressor gene. This molecular biomarker will be a powerful tool for investigating the estrogen and/or nonsteroidal estrogenic agents in controlling the etiological process of tumorigenesis in human breast and rodent mammary. It was claimed that the reduction of PTPγ expression in human breast cancer is unlikely to be due to genetic events; therefore, epigenetic mechanisms (such as methylation) might be responsible. Several genes have been demonstrated to be hypermethylated in breast carcinomas, including HIN-1, p16, E-cadherin, BRCA1, estrogen receptor, glutathione *S*-transferase P1 (GSTP1), mammary-derived growth inhibitor (MDGI), HoxA5 and 14-3-3σ (Krop *et al*., 2001). To identify the mechanisms of PTPγ reduction in human breast cancer and PTPγ downregulation by E_2 and Z, human PTPγ promoter region analysis and investigation of hypermethylation in PTPγ need to be conducted in the future.

Our data are the first evidence to demonstrate that the PTPγ does exert its suppressor capability to inhibit or slow down the proliferation of MCF-7 cells and does have the antiestrogenic activities on human breast cancers exposed to E_2 or Z. Although the *in vivo* function of PTPγ is unknown, its reduced expression in breast carcinomas and decreased colony formation following its overexpression suggest a tumor suppressor role. If similar results can be reproduced in athymic mouse testing model, then the presence of this potential cancer suppressor gene and its protein will significantly prolong the survivability of human breast cancer patients by inhibiting or slow down the proliferative ability of human breast cancer cells. The signaling pathway with PTPγ involvement may provide a new target for cancer prevention and treatment. In the future, PTPγ might be able to be applied in clinical trials for cancer prevention and cancer therapy.

Materials and methods

Cell culture

The human breast cancer cell line MCF-7 cells were purchased from American Type Culture Collection (ATCC, Manassas, VA, USA). The cells were maintained in a mixture of Dulbecco's modified Eagle's medium and Ham's F12 medium (1 : 1) (DMEM/F12) without phenol red (Sigma Chemical Co., St Louis, MO, USA) supplemented with 5% fetal bovine serum (FBS) (Atlanta Biologicals, Norcross, GA, USA) and antibiotic–antimycotic (100 U/ml penicillin G sodium, 100 μg/ml streptomycin sulfate and 0.25 μg/ml amphotericin B) (GibcoBRL, Bethesda, MD, USA) and were plated separately in 75-cm² culture flasks in a humidified incubator (5% CO_2: 95% air, 37°C). The media were changed every 2 days. When the cells grew to about 85% confluence, cells were washed twice with calcium- and magnesium-free phosphate-buffered saline (PBS, pH 7.3), and then trypsinized with 0.5% trypsin–5.3 mM EDTA (GibcoBRL) in PBS for 10 min at 37°C. The trypsinization was stopped by addition of culture medium with 5% FBS. After centrifugation, the dissociated cells were resuspended in the same medium and subcultured into 75-cm² culture flasks at a ratio of 1 : 5 flasks.

Transfection

The expression vector pCR®3.1 (Invitrogen, Carlsbad, CA, USA), containing a human full-length PTPγ cDNA (5.3 kb) in an *Eco*RI site or a partial PTPγ cDNA fragment (756 bp amplified using the following primer set: 5′-CGTCAC-CAGTCTCCTATTGA-3′ and 5′-GTCTGTCATGTCGTG-GTTCC-3′) cloned in pCR®3.1 vector. Clones containing the construct in the sense or antisense orientation were selected and used for transfection (Sorio *et al*., 1995, 1997). As a control, we used an empty pCR®3.1 vector (mock). Plasmids (10 μg) were transfected into MCF-7 cells by using Superfect (Qiagen, Valencia, CA, USA) according to the manufacturer's instructions. At 48 h after transfection, the cells were transferred to selection medium containing different doses (0, 100, 200, 400, 600, 800, 1000 μg/ml) of G-418 (Geneticin) (Invitrogen, Carlsbad, CA, USA) for 6 days to determine the optimal dose of G-418 for the selection. Finally, surviving single colonies from four to five dishes with selection medium containing 800 μg/ml of G-418 were picked from each stably transfected group for future culture and cells were treated with 400 μg/ml of G-418 in the culture medium every two to three passages to maintain the homogeneity of the cells.

RNA isolation and reverse transcription–polymerase chain reaction (RT–PCR)

A total of 1.5×10^5 viable cells from each single colony were plated in one well of six-well plates with 5 ml of culture medium and cultured to ~85% confluency. Total RNA was isolated in 1 ml of TRIZOL® Reagent (GibcoBRL) according to the manufacturer's instructions. RT–PCR was performed in a gradient mastercycler (Eppendorf®). PCR conditions were optimized for $MgCl_2$ concentration, annealing temperature and cycle number for the amplification of each of the PCR products. Under optimal conditions, the amounts of PCR products generated fell within the linear portion of the PCR amplification curve between 26 and 39 amplification cycles. Briefly, 1 μg of total RNA from cultured cells or tissues was reverse transcribed with 200 U M-MLV Reverse Transcriptase (GibcoBRL) at 42°C for 1 h in the presence of 5 mM each of dATP, dCTP, dGTP and dTTP, 4 μl 5× first-strand buffer (GibcoBRL), 0.01 M DDT, 1 U RNA Guard RNase inhibitor (Pharmacia Biotech, Uppsala, Sweden), and 2.5 μM random hexamers in a total volume of 20 μl. The reaction was terminated by heating to 95°C for 3 min. The newly synthesized cDNAs were used as templates for PCR after adjusting reagent concentrations to 3.5 mM $MgCl_2$, 2.5 μl 10× PCR Buffer (GibcoBRL), 1 U Platinum® *Taq* DNA polymerase (GibcoBRL), and 0.24 μM primers. The reactant was incubated at 95°C for 5 min. Then, 30 cycles of amplification were performed with each cycle consisting of denaturation at 95°C for 1 min, annealing at 63°C for 1 min, and extension at 72°C for 1 min. The primer sequences generating 990 bp PCR products for full-length PTPγ construct were 5′-GTA TGG AGC AGT TTC AGC-3′ (sense at PTPγ exon 29) and 5′-TAG AAG GCA CAG TCG AGG-3′ (antisense at pCR®3.1 reverse priming site). The primer sequences generating 583 bp PCR products for antisense PTPγ construct were 5′-TAA TAC GAC TCA CTA TAG GG-3′ (sense at T7 promoter priming site in pCR®3.1 vector) and 5′-GAA CAC AGC ATC AAT GGC AGG AGG-3′ (antisense at PTPγ exon 4). The primer sequences generating 337 bp PCR products for sense PTPγ construct were 5′-TAA TAC GAC TCA CTA TAG GG-3′ (sense at T7 promoter priming site in pCR®3.1 vector) and 5′-CCT CCT GCC ATT GAT GCT GTG TTC-3′ (antisense at PTPγ exon 4). The primer sequences generating 492 bp PCR product for PTPγ were 5′-GCG CAG CGA CTT TAG CCA GAC GA-3′ (sense at PTPγ exon 8) and 5′-GCT CCC GCT CCC CAT CCT CAC TC-3′ (antisense at PTPγ exon 11). The primer sequences generating 563 bp PCR products for 36B4 were 5′-AAA CTG CTG CCT CAT ATC CG-3′ (sense at 306–325) and 5′-TTG ATG ATA GAA TGG GGT ACT GAT G-3′ (antisense at 868–848). The final PCR products (10 μl) mixed with 1 μl of 10× loading buffer were separated on a 1.5% agarose gel containing ethidium bromide. The specific bands were quantified by ImageQuaNT software (Molecular Dynamics, Sunnyvale, CA, USA). The results are presented as the ratio of each PCR product to 36B4. 36B4 is a cDNA clone for human acidic ribosomal phosphoprotein PO (Masiakowski *et al*., 1982), for which mRNA levels have been shown to be unmodified by estradiol treatment (Laborda, 1991).

Immunohistochemical staining

Wild-type MCF-7 cells (MCF-7), mock-transfected MCF-7 cells (M7-pCR®3.1-800 (s)), PTPγ-overexpressed MCF-7 cells (M7-PTPγ-800 (s)), antisense PTPγ-transfected MCF-7 cells (M7-A24-800 (s)) and sense PTPγ-transfected MCF-7 cells (M7-B19-800 (s)) were cultured on 24 × 30 mm cell culture cover slips (Cat. No: 150067, Nalge Nunc Int., Naperville, IL, USA) and washed in PBS for three times. After −10°C methanol fixation for 5 min and air-dry, cells were stained for PTPγ by using VECTASTAIN® Universal Quick Kit and DAB Substrate Kit (Cat. No. PK-8800, Cat. No. SK-4100, Vector Laboratories, Inc., Burlingame, CA, USA) according to the manufacturer's instructions. The primary antibody was an affinity-purified rabbit polyclonal antibody raised against a self-designed in-house synthetic peptide (N-SEDGERE-HEEDGEKD-C) corresponding to amino acids 588–602 mapping in the extracellular domain of the PTPγ precursor of human origin and was produced by Sigma® Genosys (The Woodlands, TX, USA). An optimal primary antibody dilution of 1 : 100 was determined by titration in this system, and omission of primary antibody served as a negative control.

Doubling time assay

Wild-type MCF-7 cells, M7-pCR®3.1-800 (s), M7-PTPγ-800 (s), M7-A24-800 (s) and M7-B19-800 (s) were plated separately at a density of 0.5×10^4 cells/well in 24-well plates in a volume of 1 ml/well. After cells are attached to the wells, the medium was replaced with 2 ml of fresh DMEM/F12 with 5% FBS. At the same time (time 0 h), a group of cells were counted. Cells were grown for 3 days and counted every 8 h. Adherent cells were detached by rapid trypsinization. An adequate volume of medium containing trypan blue was added. Then cells were counted by using a hemacytometer. Experiments were performed in four replicate wells, and each experiment was repeated twice. Based on the counted cell numbers at different time points, a cell proliferation curve was generated. Cell doubling (CD) was calculated by using the formula: $\ln(N_j - N_i)/\ln 2$, where N_j or N_i is the cell numbers at different time point T_j or T_i ($T_j > T_i$) in the growth log phase of the cells. Doubling time (DT) was consequently obtained by dividing the time interval ($T_j > T_i$) by CD (Poliseno *et al*., 2002).

Soft agar assay for colony formation

Cells were cultured in six-well plates first covered with an agar layer (phenol red-free DMEM/F12 with 0.5% agar and 10% FBS. The middle layer contained different number of cells (2000, 4000, 8000 or 16 000 cells) in phenol red-free DMEM/F12 with 0.35% agar and 10% FBS. The top layer, consisting of medium, was added to prevent drying of the agar in the plates. The plates were incubated for 21 days, after which the plates were stained in 0.5 ml of 0.005% crystal violet for >1 h and the cultures were inspected and photographed. Colony efficiency (CE) was determined by a count of the number of colonies greater than 15 μm in diameter, which was calculated as the average of colonies counted at ×50 magnification in five individual fields by using BioQuant NOVA software.

Nonradioactive cell proliferation assay

A total of 2×10^4 cells (Wild type MCF-7 cells, M7-pCR®3.1-800 (s), M7-PTPγ-800 (s), M7-A24-800 (s) or M7-B19-800 (s)) were seeded and cultured in each well of 24-well plates in phenol red-free high-calcium DMEM/F12 supplemented with 5% FBS overnight. The medium was switch to phenol red-free high-calcium DMEM/F12 supplemented with Dextran-coated charcoal (DCC) (Dextran T-70, Pharmacia; activated charcoal, Sigma)-stripped FBS (5%). After 24 h, cells were treated with the E_2 or Z at 0, 7.5, 15, 30, 60 or 120 nM in the same fresh medium for 24 h. Cell proliferation rate was quantified by using CellTiter 96™ AQueous assay (Promega, Madison, WI, USA). Briefly, at the end of treatment, the medium in the wells were discarded and 250 μl of fresh medium with 50 μl of freshly combined MTS/PMS (the ratio of MTS : PMS is 20 : 1))

solution was added to each well. Then, the plates were incubated for 1.5 h and the color density was checked every 30 min. Finally, 100 μl of culture medium from each well were transferred to one well of 96-well plates and optical density was read at 490 nm ($OD_{490\,nm}$) by an ELISA plate reader.

Statistical analysis

The results for DT assay and nonradioactive cell proliferation assay were presented as the mean $\pm$ standard deviation (s.d.) for four replicate culture wells as one group. The results for colony efficiency assay were presented as the mean $\pm$ s.d. for five individual fields as one well. Analysis was performed using Minitab statistical software for Windows (Minitab Inc., State College, PA, USA). Statistical differences were determined by using one-way ANOVA for independent groups. *P*-values of less than 0.05 were considered to be statistically significant.

Acknowledgements
This study was supported by Department of Defense Breast Cancer Research Program Grants DAMD 8140 and 9341, and NIH Grants CA 94718 and CA 95915. MIUR 60%, Fondazione Cassa di Risparmio di Verona (Bando 2001) and Consorzio per gli Studi Universitari in Verona, Italy. We thank Dr Kay Huebner for the critical reading of this manuscript.

References

Barnea G, Silvennoinen O, Shaanan B, Honegger AM, Canoll PD, D'Eustachio P, Morse B, Levy JB, LaForgia S, Huebner K, Musacchio JM, Sap J and Schlessinger J. (1993). *Mol. Cell. Biol.*, **13,** 1497–1506.

Gaits F, Li RY, Ragab A, Ragab-Thomas JMF and Chap H. (1995). *Biochem. J.*, **311,** 97–103.

Kaplan R, Morse B, Huebner K, Croce C, Ravera M, Ricca G, Jaye M and Schlessinger J. (1990). *Proc. Natl. Acad. Sci. USA*, **87,** 7000–7004.

Klarlund JK. (1985). *Cell*, **41,** 707–717.

Krop IE, Sgroi D, Porter DA, Lunetta KL, LeVangie R, Seth P, Kaelin CM, Rhei E, Bosenberg M, Schnitt S, Marks JR, Pagon Z, Belina D, Razumovic J and Polyak K. (2001). *Proc. Natl. Acad. Sci. USA*, **98,** 9796–9801.

Krueger NX and Saito H. (1992). *Proc. Natl. Acad. Sci. USA*, **8,** 7417–7421.

Krueger NX, Streuli M and Saito H. (1990). *EMBO J.*, **9,** 3241–3252.

Kulp SK, Liu S, Sugimoto Y, Brueggemeier RW and Lin YC. (2000). *Biol. Reprod.*, **62** (Suppl 1), 181–182.

Laborda J. (1991). *Nucleic Acids Res.*, **19,** 3998.

LaForgia S, Lasota J, Latif F, Boghosian-sell L, Kastury K, Ohta M, Druck T, Atchison L, Cannizzaro L, Barnea G, Schlessinger J, Modi W, Kuzmin I, Tory K, Zbar B, Croce CM, Lerman M and Huebner K. (1993). *Cancer Res.*, **53,** 3118–3124.

LaForgia S, Morse B, Levy J, Barnea G, Cannizzaro LA, Li F, Nowell PC, Boghosian-sell L, Glick J, Weston A, Harris CC, Drabkin H, Patterson D, Crose CM, Schlessinger J and Huebner K. (1991). *Proc. Natl. Acad. Sci. USA*, **88,** 5036–5040.

Levy JB, Canoll PD, Silvennoinen O, Barnea G, Morse B, Honegger AM, Huang J-T, Cannizzaro LA, Park S-H, Druck T, Huebner K, Sap J, Ehrlich M, Musacchio JM and Schlessinger J. (1993). *J. Biol. Chem.*, **268,** 10573–10581.

Lin YC, Chang CJG, Sugimoto Y, Chen R, Canatan H, Brueggemeier RW and Dayton MA. (1994). *Proceedings of the American Association for Cancer Research 85th Annual Meeting*, Vol. 35, 607a (Abstract #3619).

Liu S, Kulp SK, Sugimoto Y, Jiang J, Chang HL and Lin YC. (2002). *Breast Cancer Res. Treat.*, **71,** 21–35.

Lubinski J, Hadaczek P, Podolski J, Toloczko A, Sikorski A, McCue P, Druck T and Huebner K. (1994). *Cancer Res.*, **54,** 3710–3713.

Masiakowski P, Breathnach R, Bloch J, Gannon F, Krust A and Chambon P. (1982). *Nucleic Acids Res.*, **10,** 7895–7903.

Poliseno L, Mariani L, Collecchi P, Piras A, Zaccaro L and Rainaldi G. (2002). *Cancer Chemother. Pharmacol.*, **50,** 127–130.

Shock LP, Bare DJ, Klinz PF and Maness PF. (1995). *Mol. Brain Res.*, **28,** 110–116.

Sorio C, Melotti P, D'Arcangelo D, Mendrola J, Calabretta B, Croce CM and Huebner K. (1997). *Blood*, **90,** 49–57.

Sorio C, Mendrola J, Lou Z, Laforgia S, Croce CM and Huebner K. (1995). *Cancer Res.*, **55,** 4855–4864.

Tsukamoto T, Takahashi T, Ueda R, Hibi K, Saito H and Takahashi T. (1992). *Cancer Res.*, **51,** 3506–3509.

van Niekerk CC and Poels LG. (1999). *Cancer Lett.*, **137,** 61–73.

Zheng J, Kulp SK, Zhang Y, Sugimoto Y, Dayton MA, Govindan MV, Brueggemeier RW and Lin YC. (2000). *Anticancer Res.*, **20,** 11–20.